The Advanced LIGO Detectors in the Era of First Discoveries

Benno Willke

for the LIGO scientific collaboration (LSC)

LIGO-G1601139

Leibniz Universität Hannover

and

Max-Planck-Institut für Gravitationsphysik

(Albert-Einstein-Institut)

Gravitational Wave Transducer

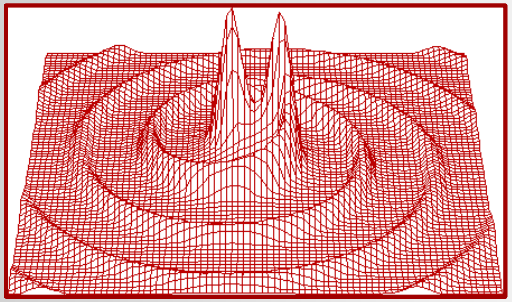

GW strain $h(t)$ → **Gravitational Wave Transducer** (Advanced LIGO) → *discrete digital representation of strain* $H(t_k)$

Gravitational Wave Transducer

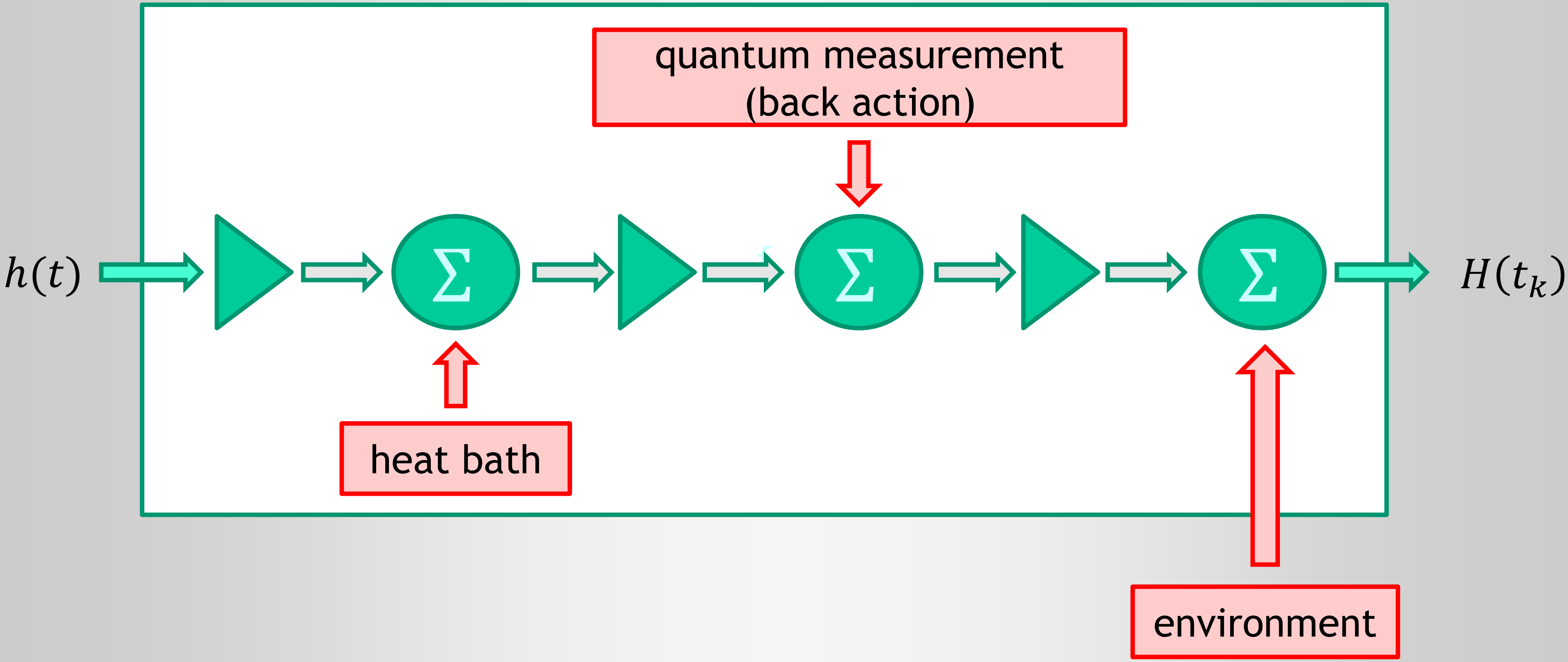

Interferometer Response to GW

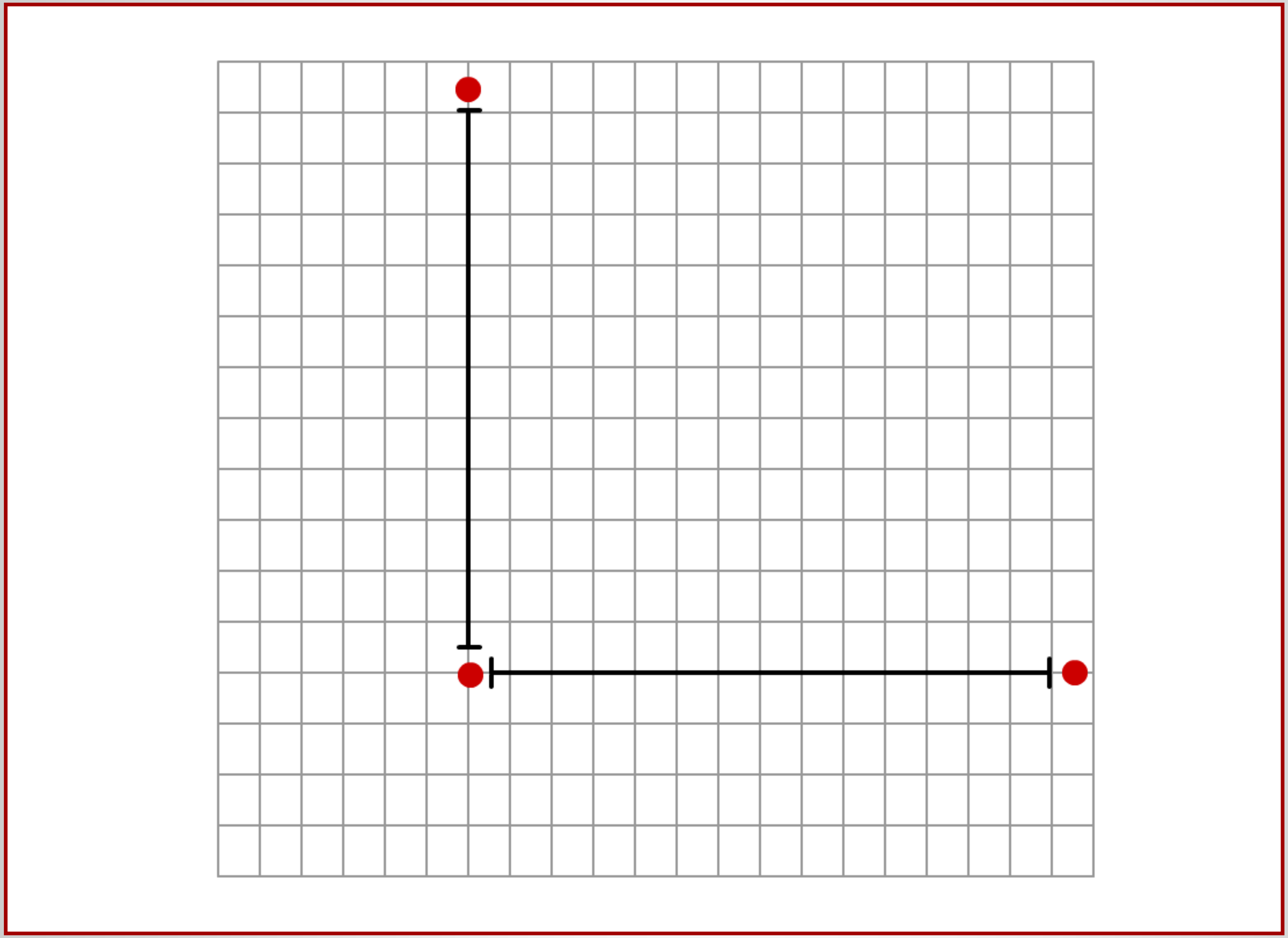

credit: Patrick Kwee, AEI

Interferometer Response to GW

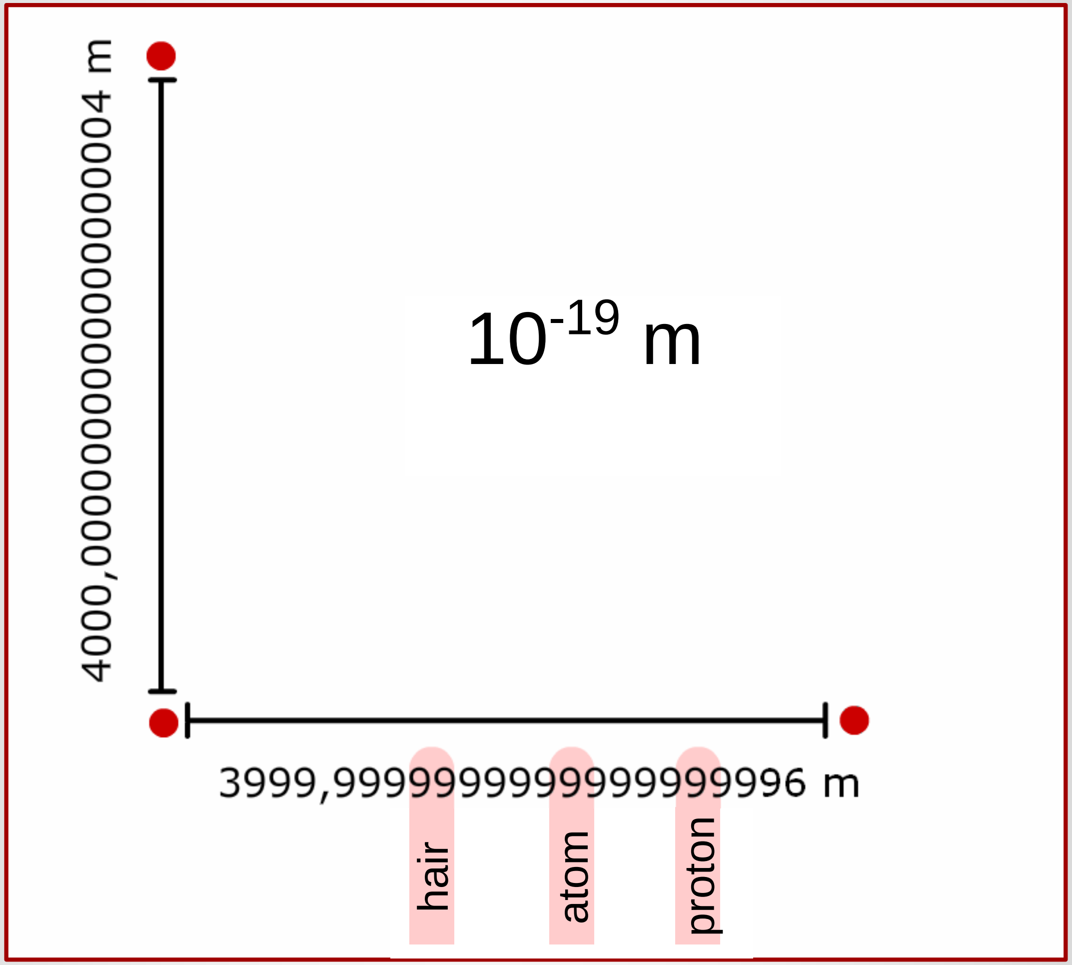

credit: Patrick Kwee, AEI

Interferometer Response to GW

$$h = \frac{2\delta l}{l} \le 10^{-22}$$

$$\delta l = \frac{h}{2} l \qquad \delta\varphi = \frac{2\pi h}{\lambda} l$$

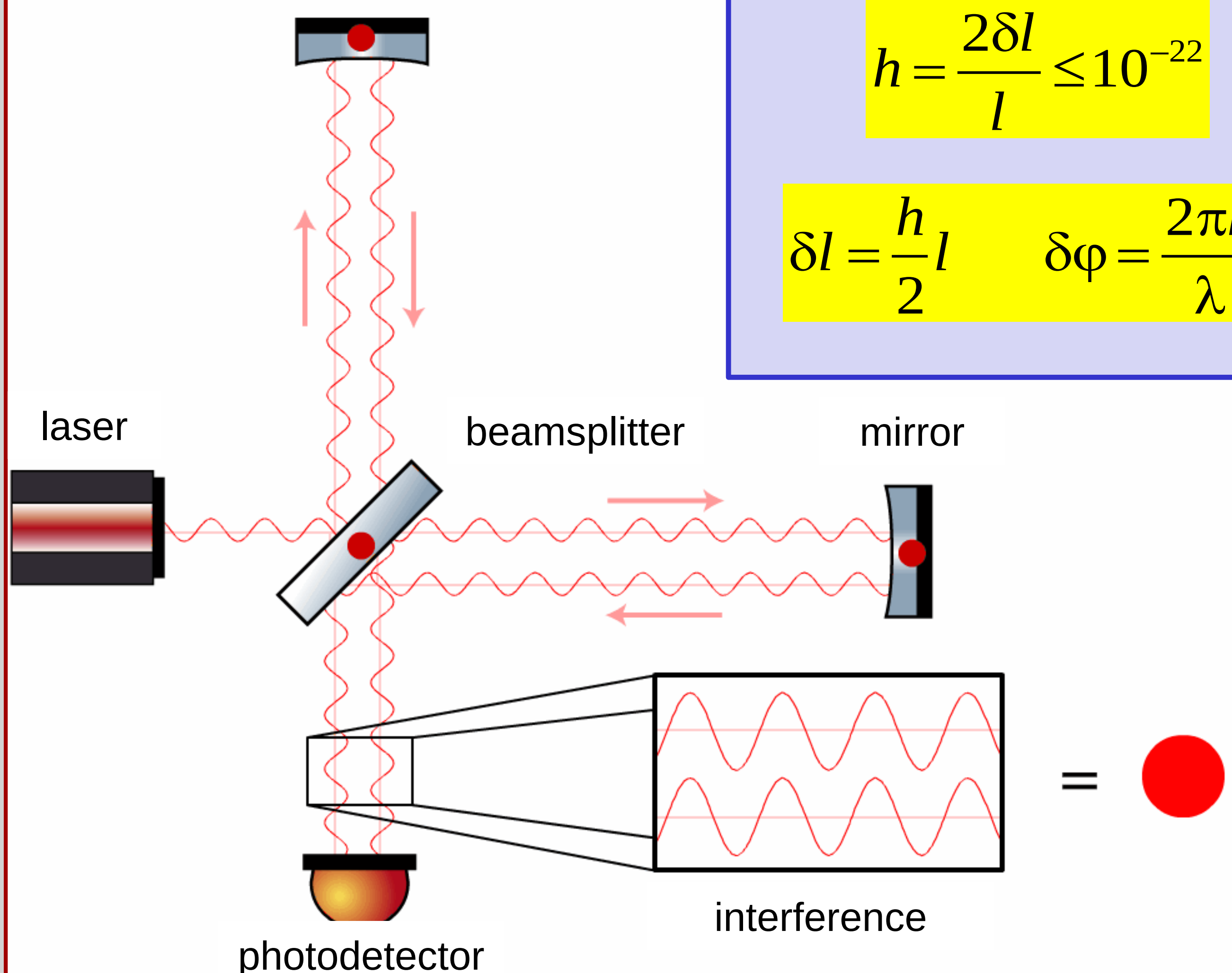

credit:
Patrick Kwee, AEI

Interferometer with „Free“ Mirrors

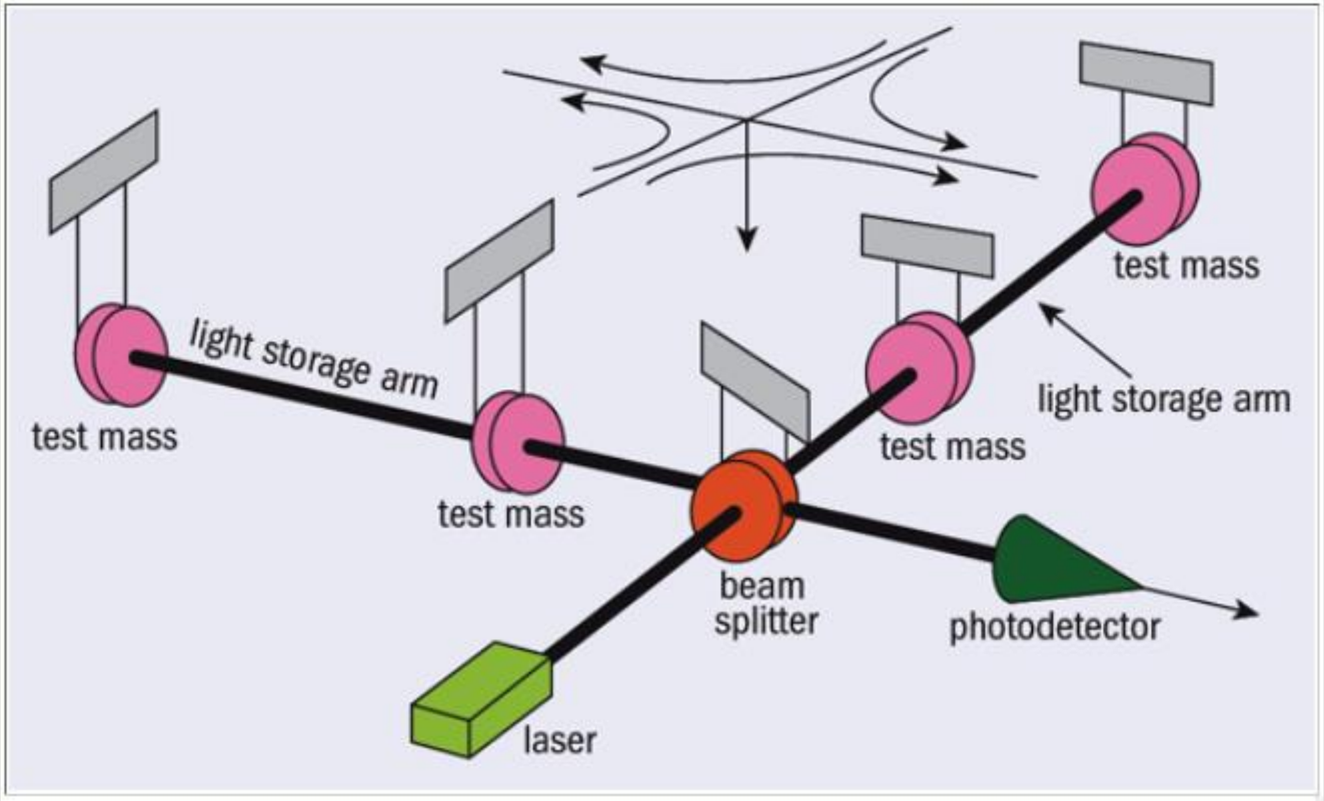

credit: CERN courrier

aLIGO Noise Sources - Spectral Density

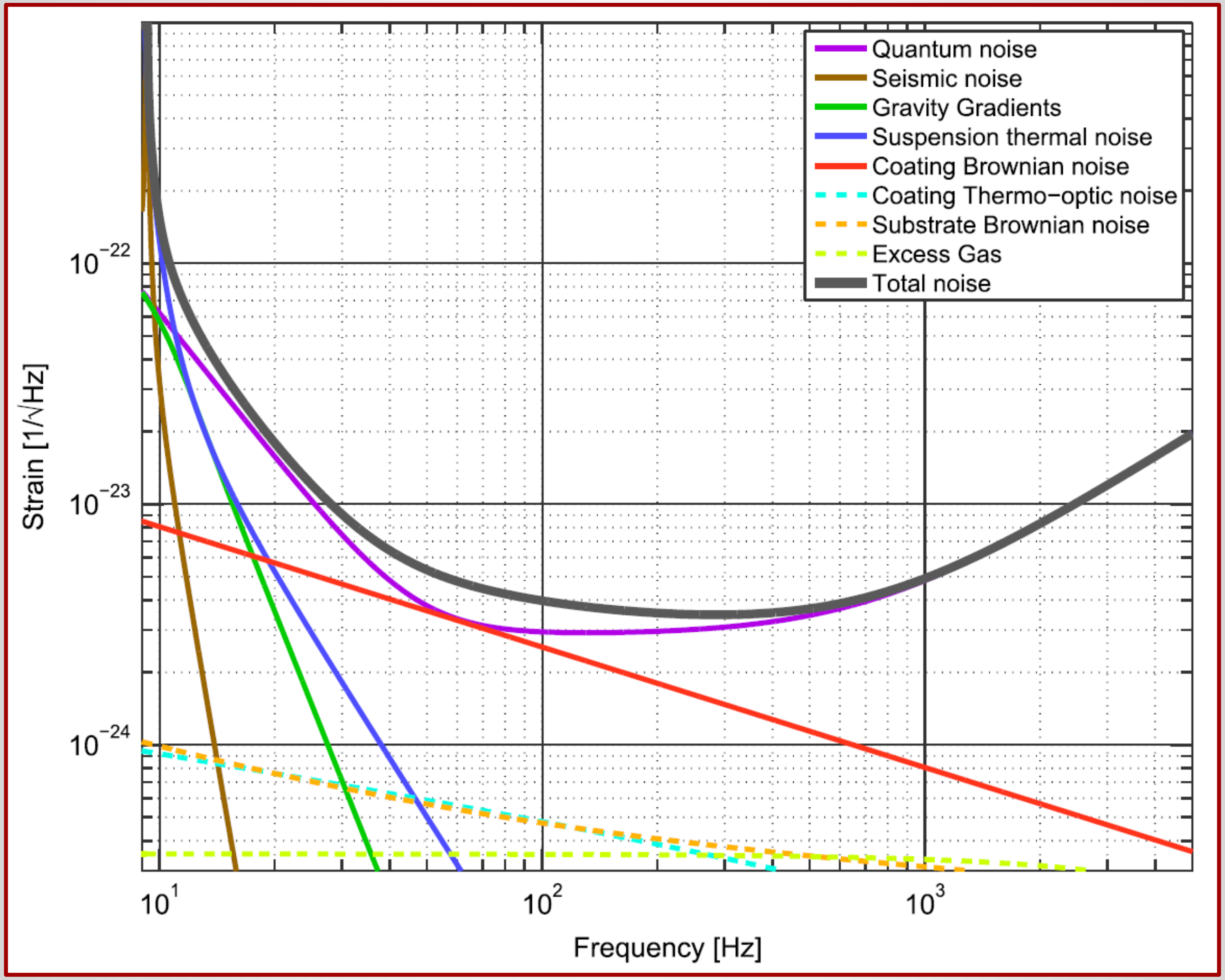

Aasi et al., Class. Quantum Grav. 32 (2015) 074001

Gravitational Wave Transducer

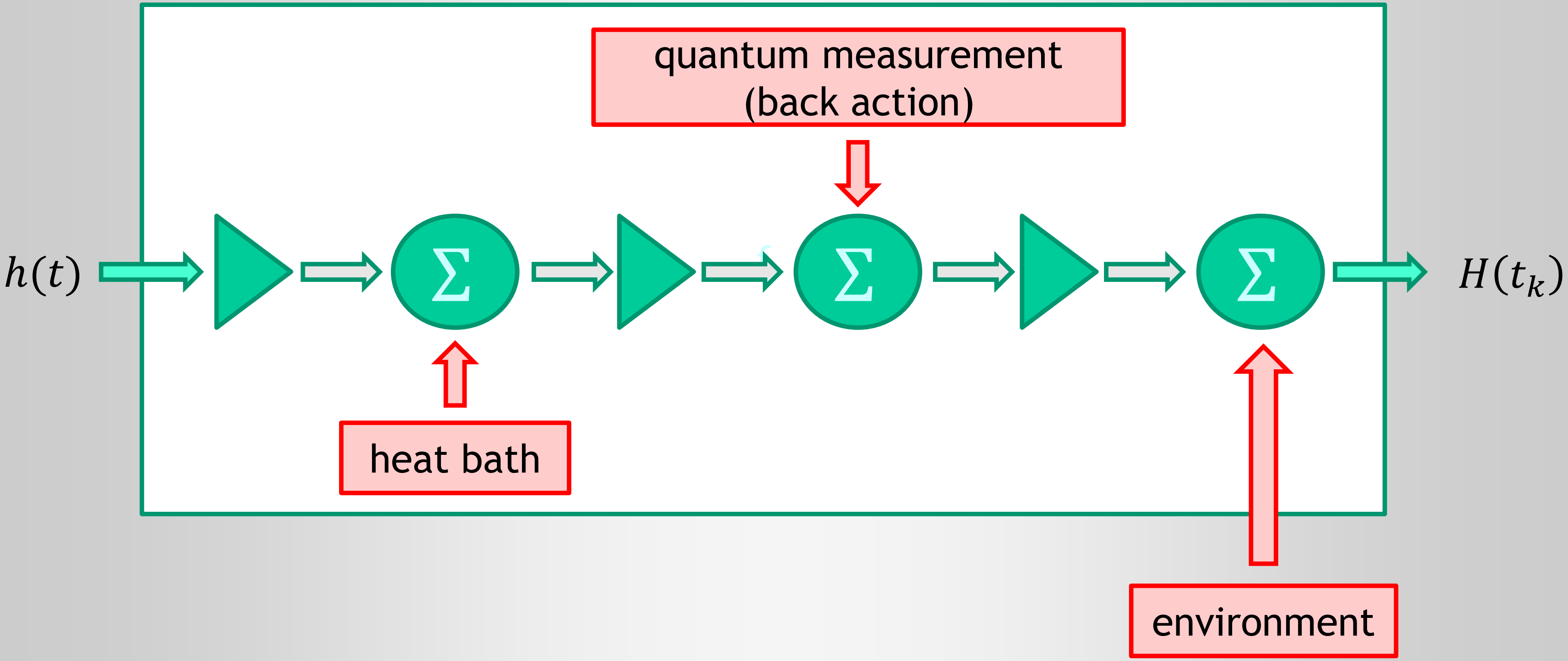

Interferometer Response to GW

$$h = \frac{2\delta l}{l} \leq 10^{-22}$$

$$\delta l = \frac{h}{2} l \qquad \delta\varphi = \frac{2\pi h}{\lambda} l$$

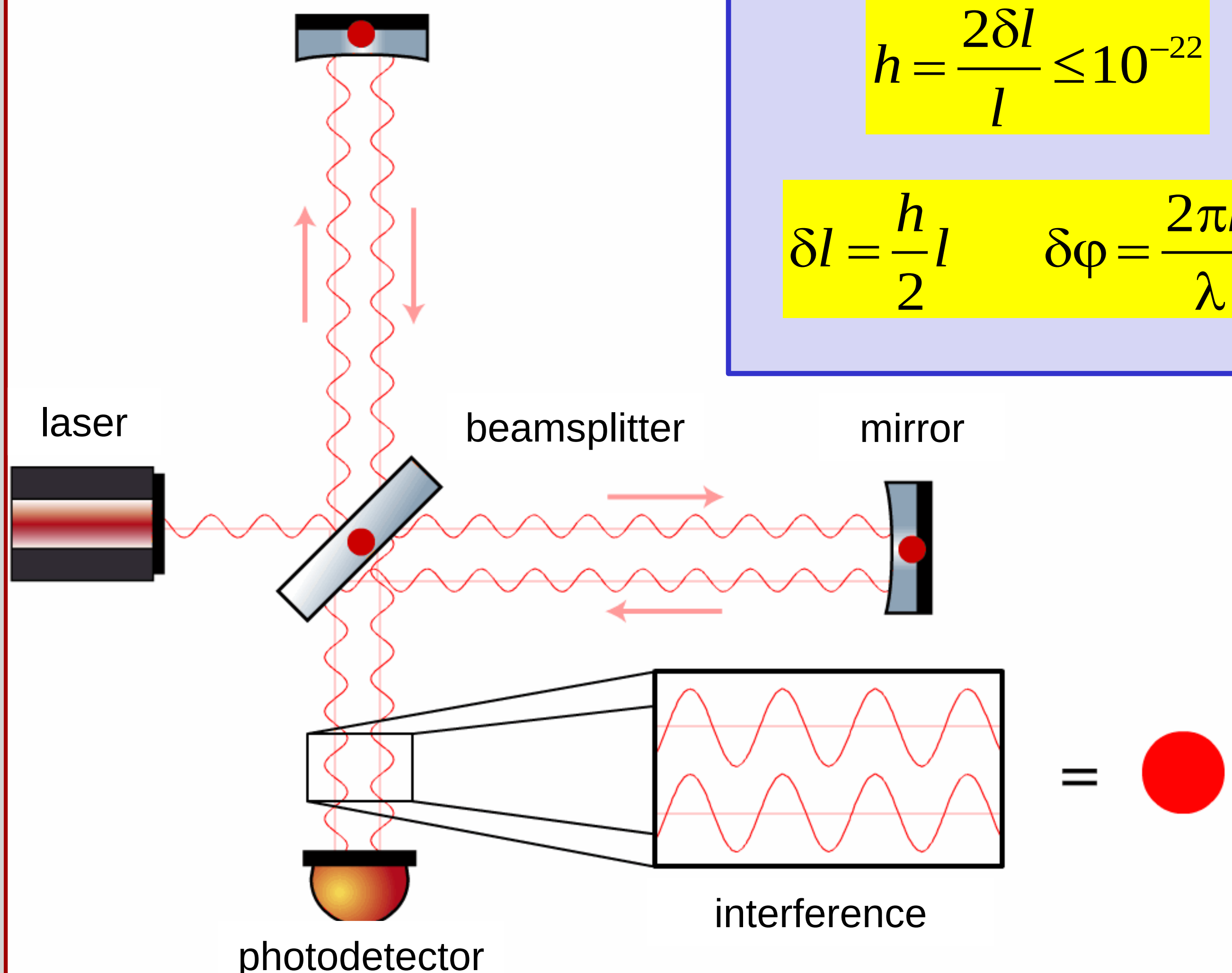

credit:
Patrick Kwee, AEI

Michelson IFO at mid-fringe

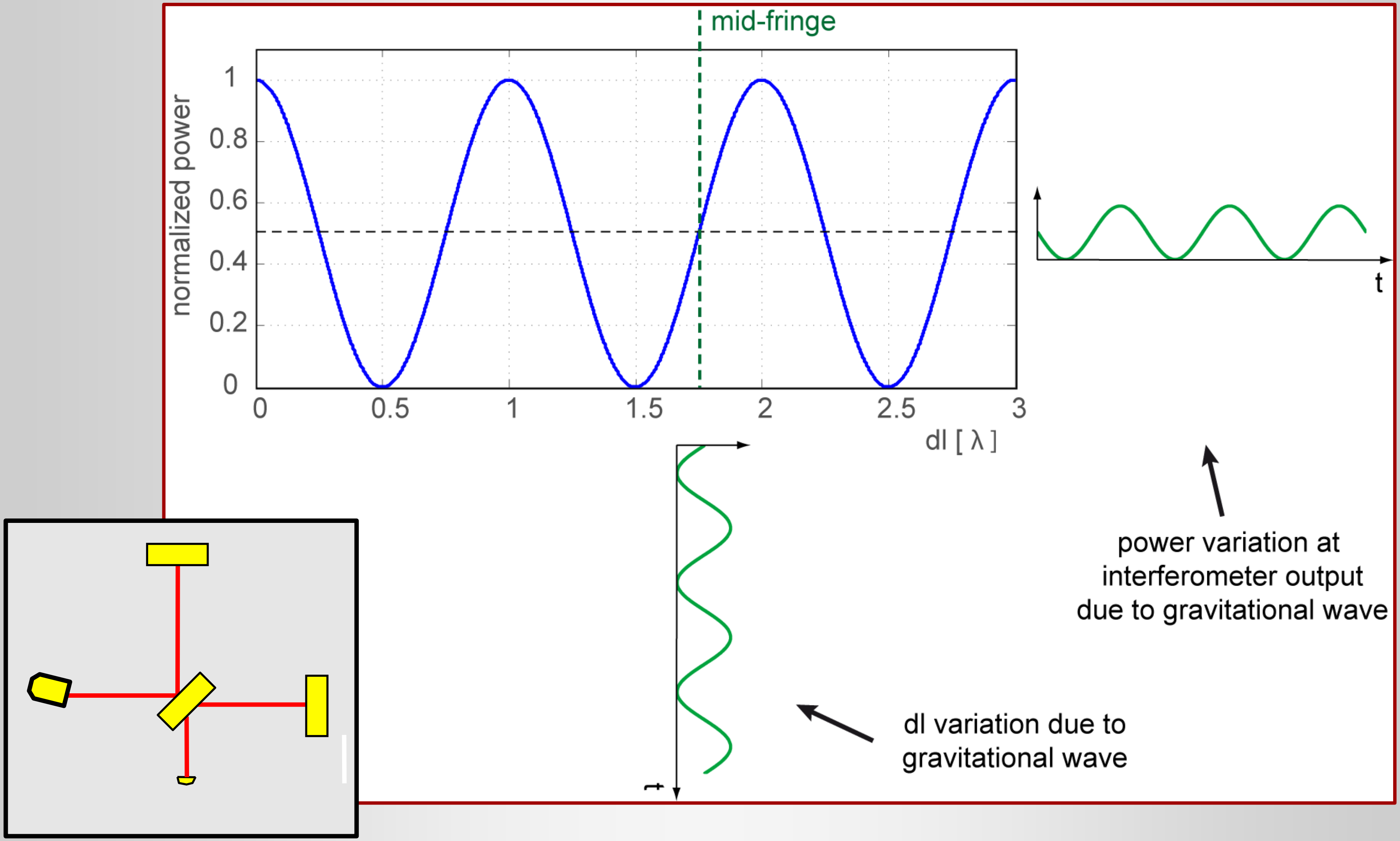

Michelson IFO With Varying Intensity

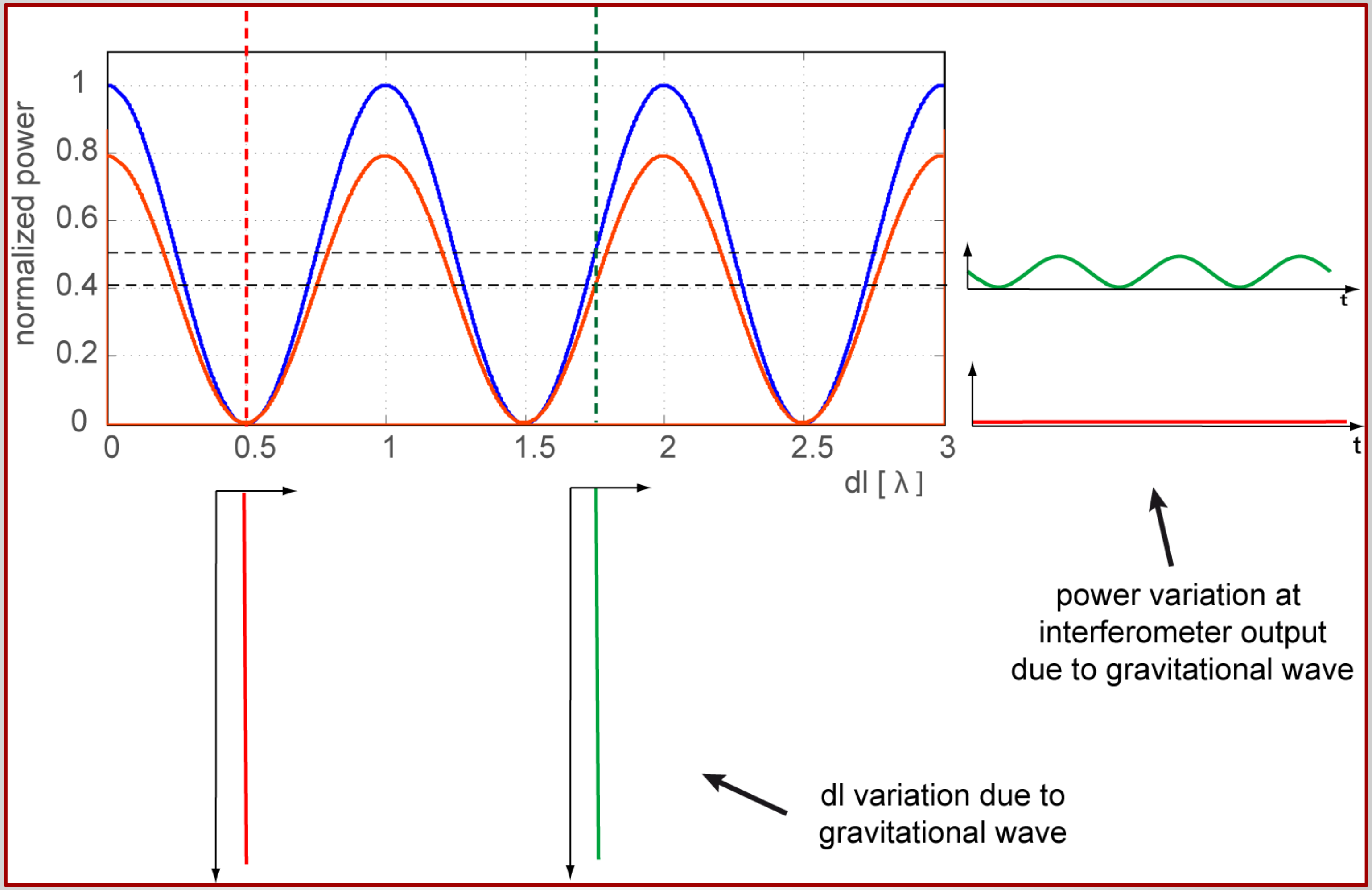

Phasor Picture

- define $E = \Re(A)$ with $A(z,t) = a \cdot exp\big(i(\omega t - kz)\big)$
- plot $a = E_0(t) \cdot \exp(i\varphi_s(t))$ as a vector in complex plane
- use basepoint of vector to identify frequency on second horizontal axis

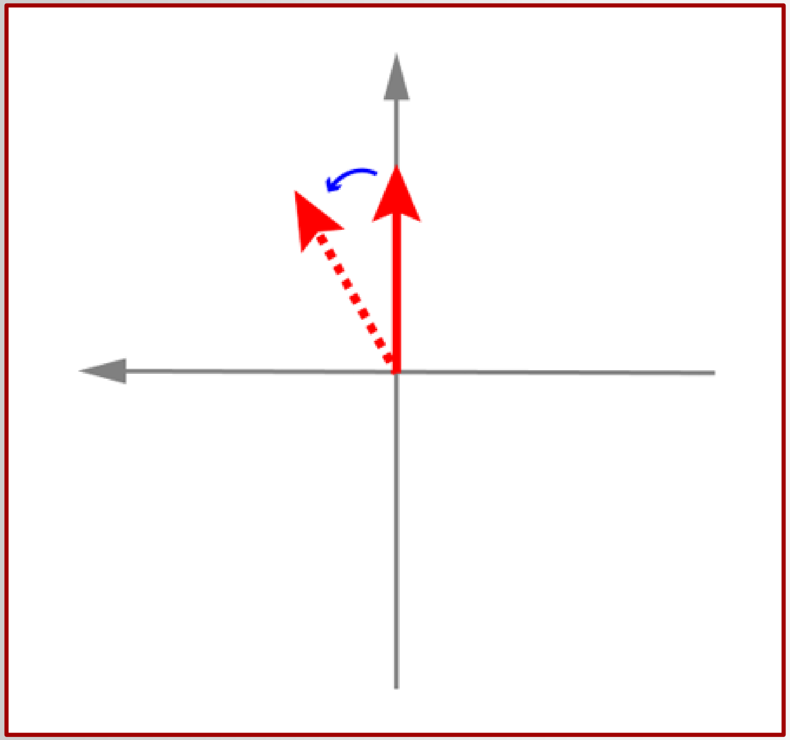

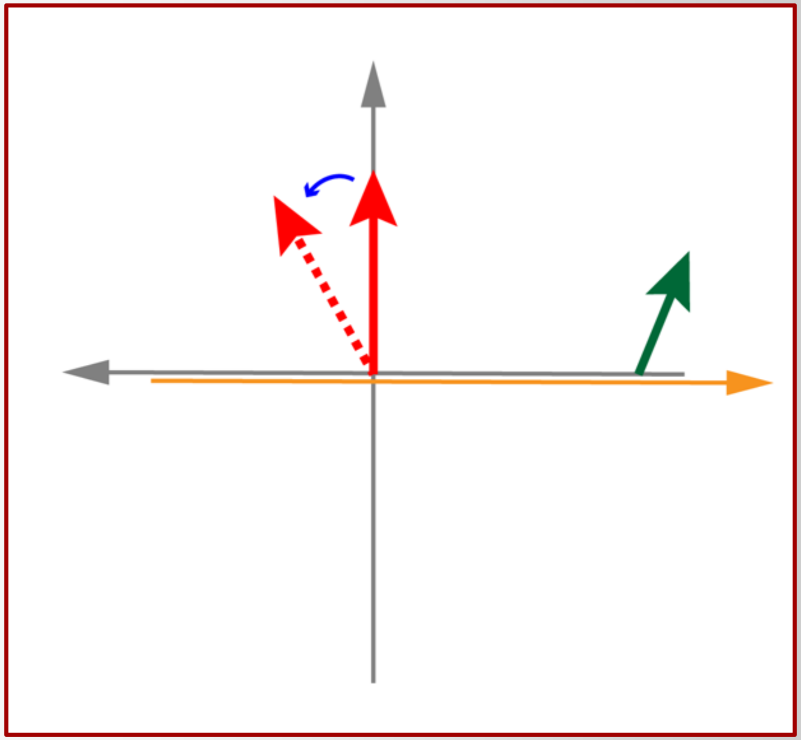

Dark Fringe Operation Point

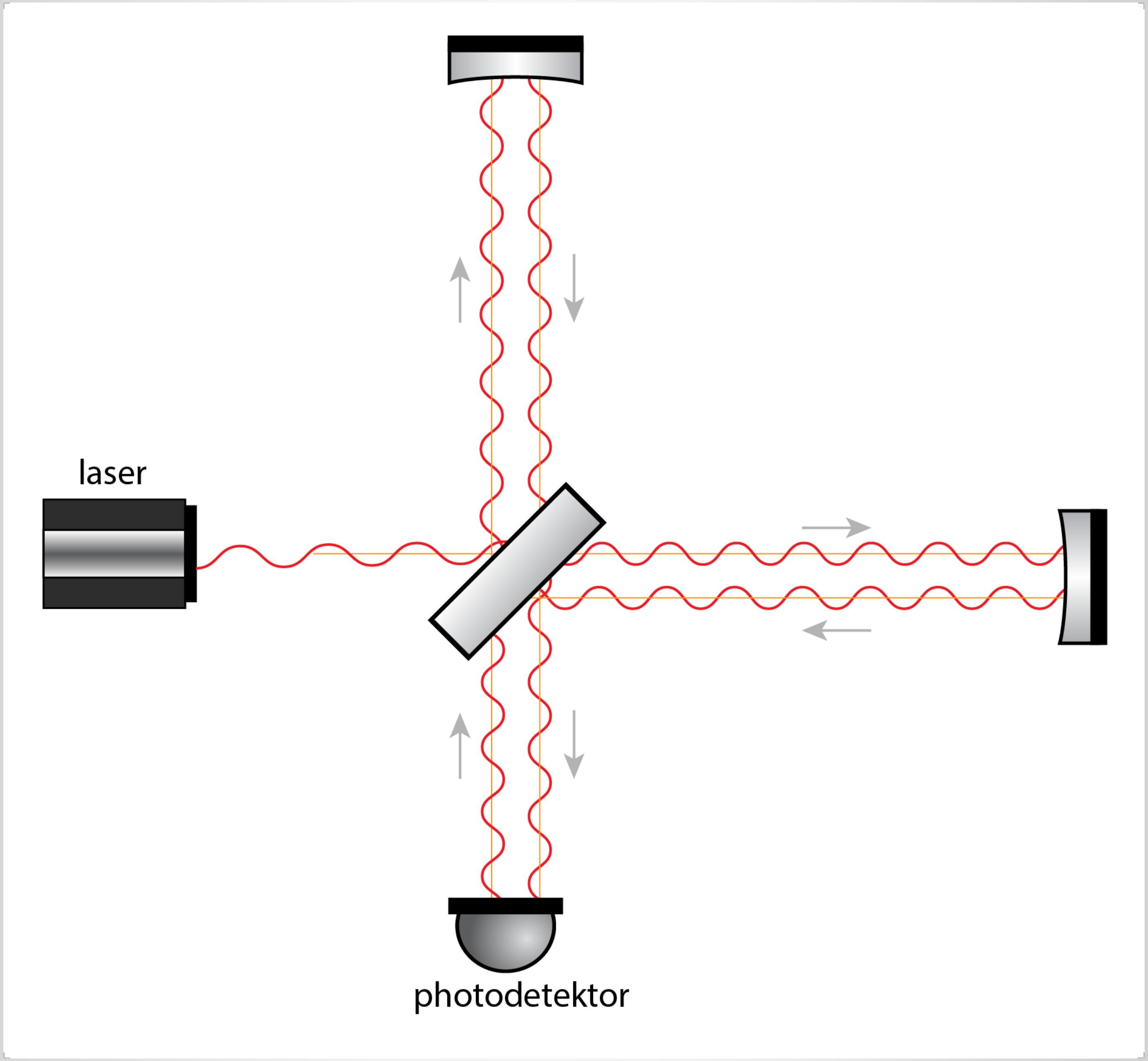

Dark Fringe Operation Point

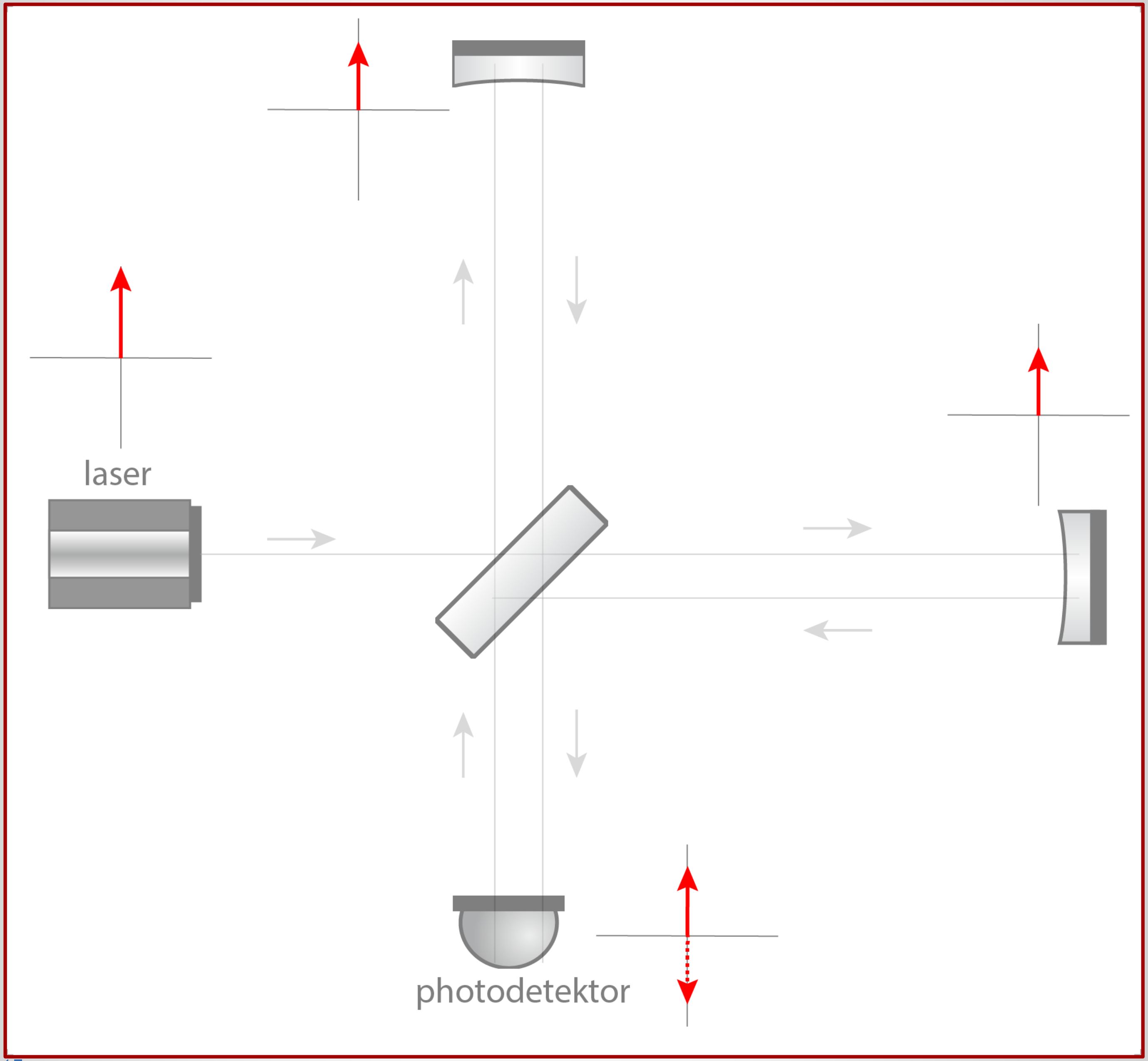

Differential Phase Change in Arms

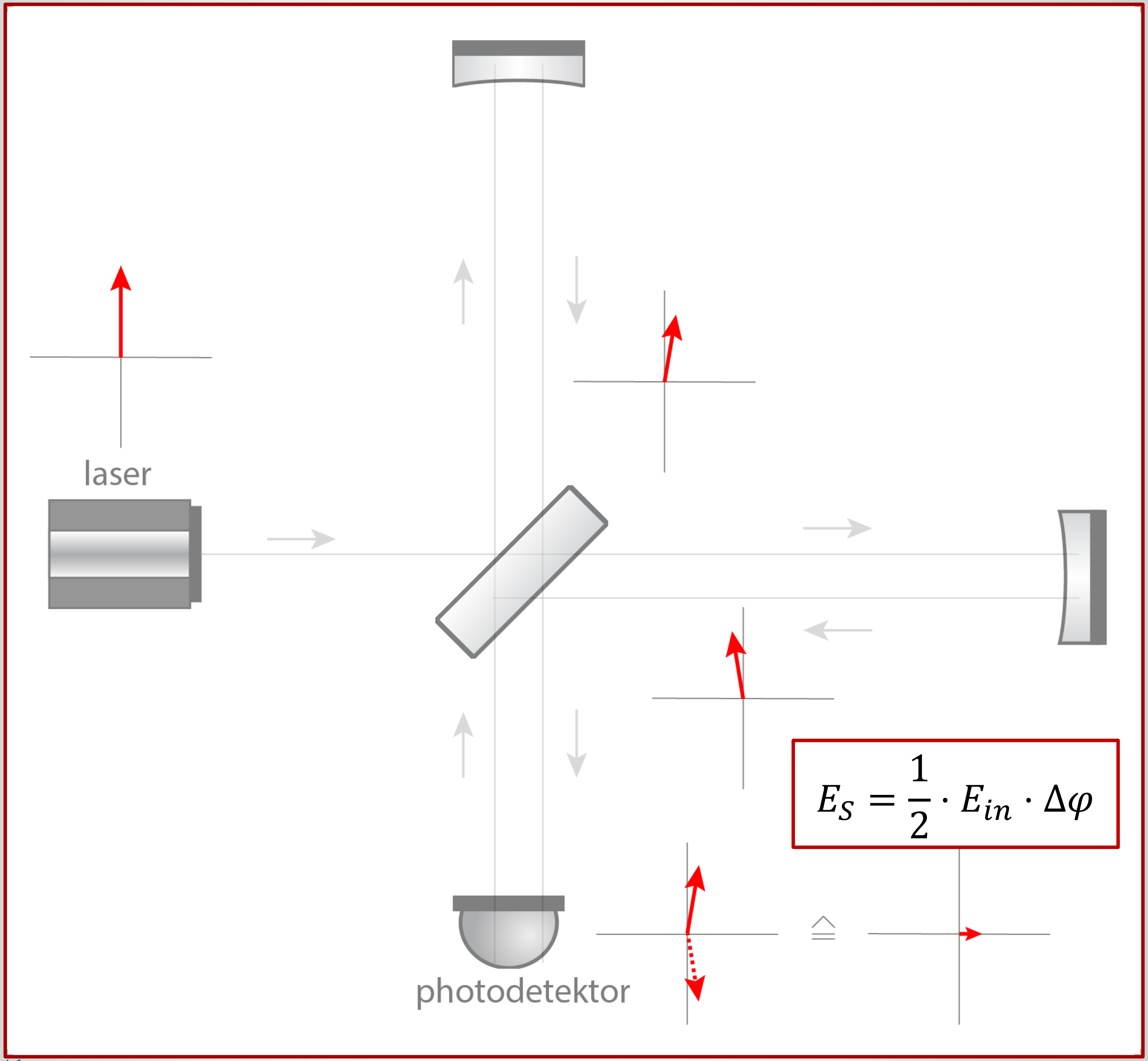

$$E_S = \frac{1}{2} \cdot E_{in} \cdot \Delta\varphi$$

Accumulated Phase Shift in Arm Cavities

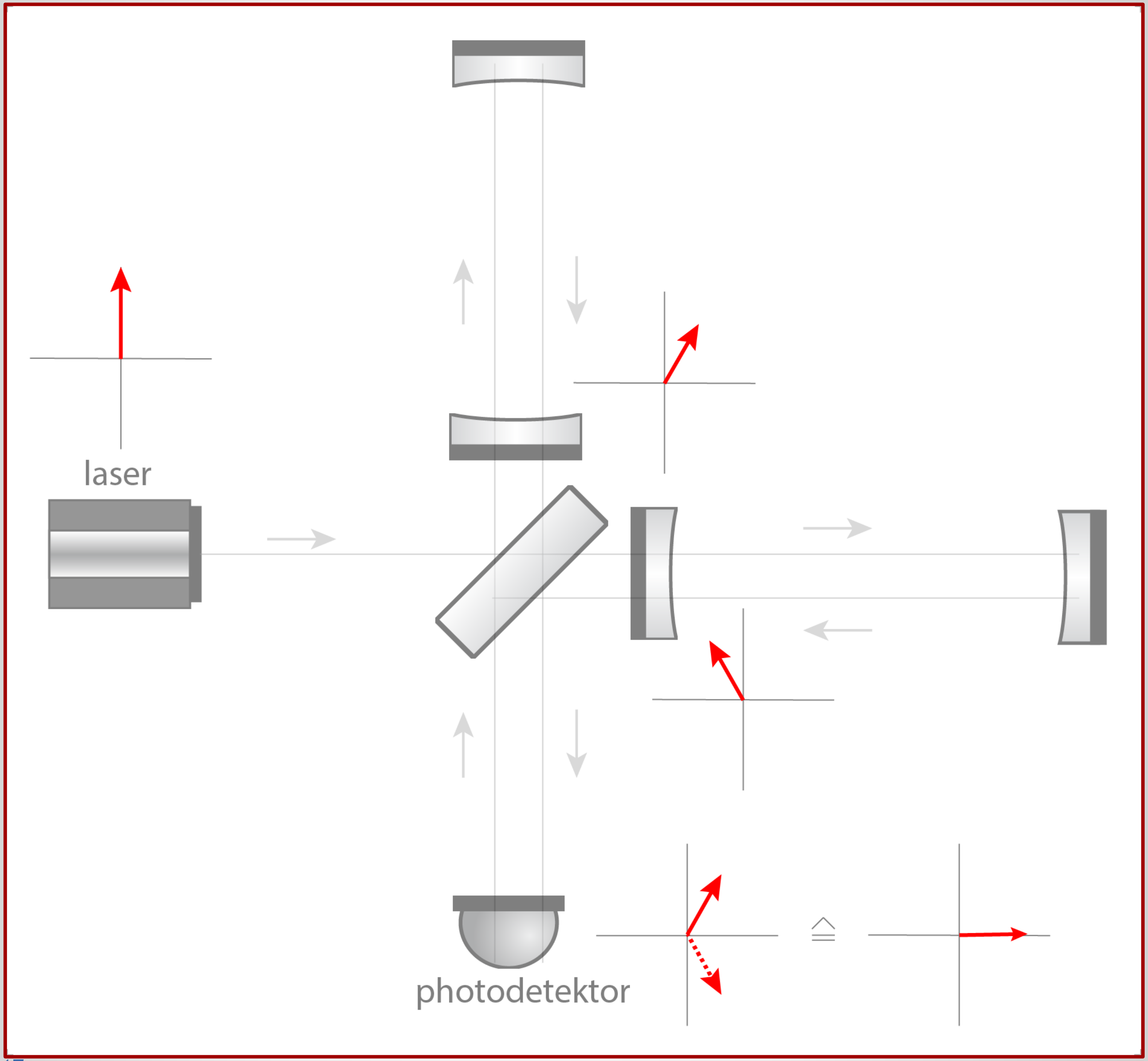

Leibniz Universität Hannover

Gravitational Wave Transducer

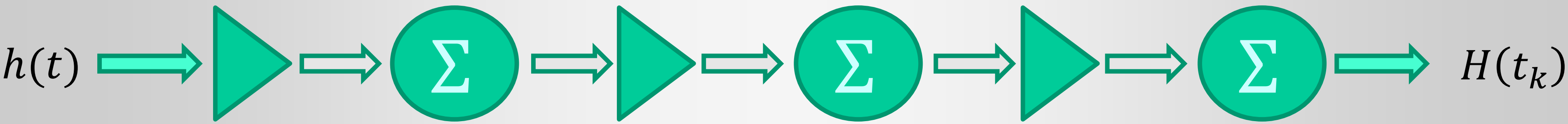

frequency domaint description:

$$H(f) = C(f) \cdot h(f)$$

optical responce (optical gain)

$$C(f) = \frac{4\pi \cdot G_{arm} \cdot L_0}{\lambda} \left(\frac{G_{prc} \cdot P_{in} \cdot P_{LO}}{G_{src}} \right)^{1/2} \cdot K_{-}(f)$$

$K_{-}(f)$: differential coupled cavity pole

Martynov D.V. et al., arXiv:1604.00439 [astro-ph.IM]

Gravitational Wave Transducer

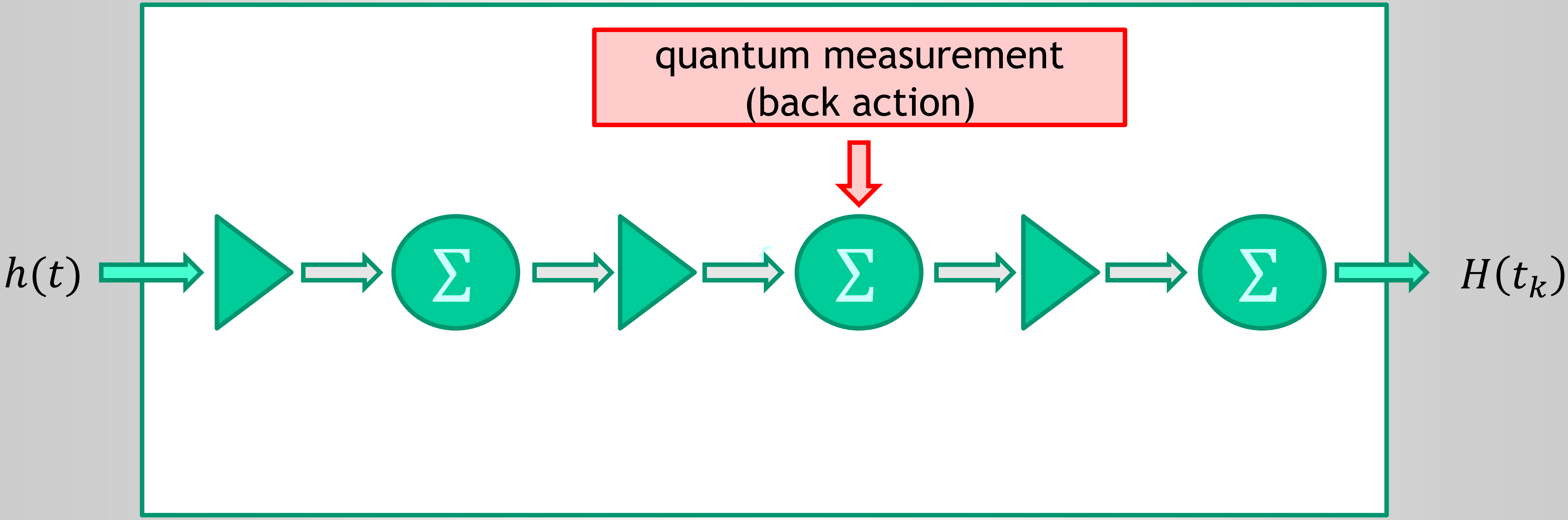

Sinusoidal Phase Shift in Arms – Sideband Picture

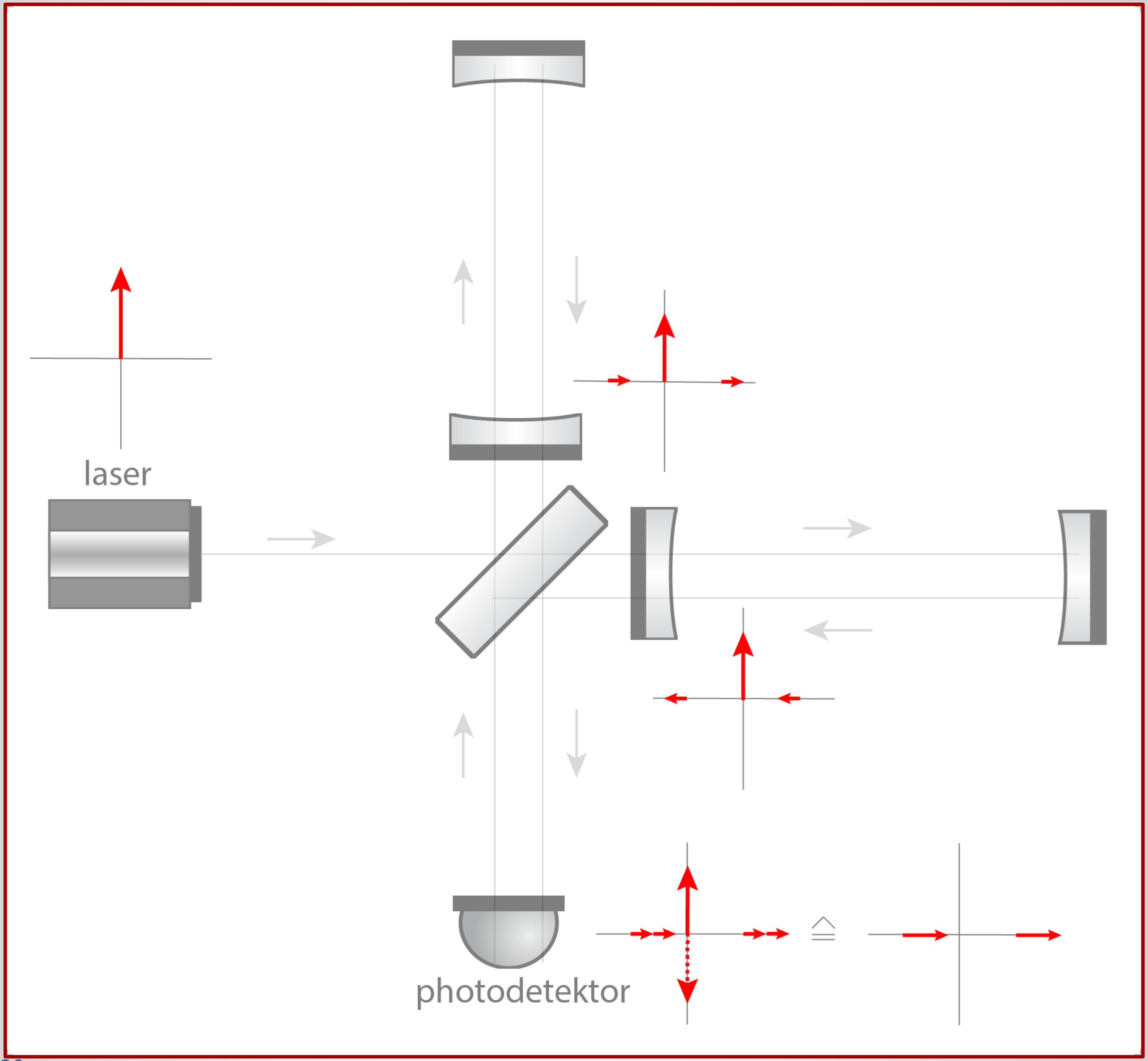

Quantum Vacuum Fluctuations – Two Quadratures

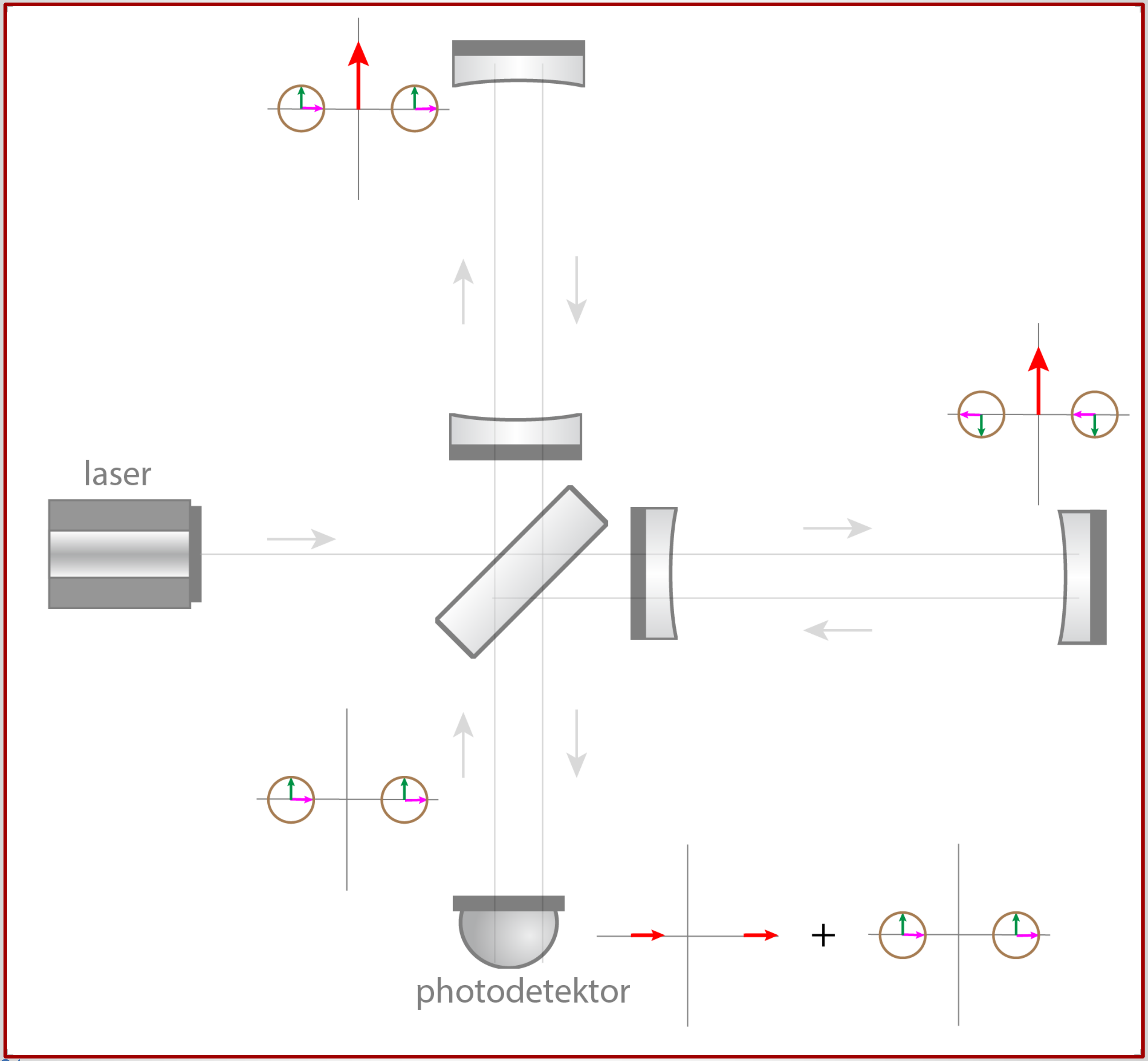

Quantum Vacuum Fluctuations – Radiation Pressure

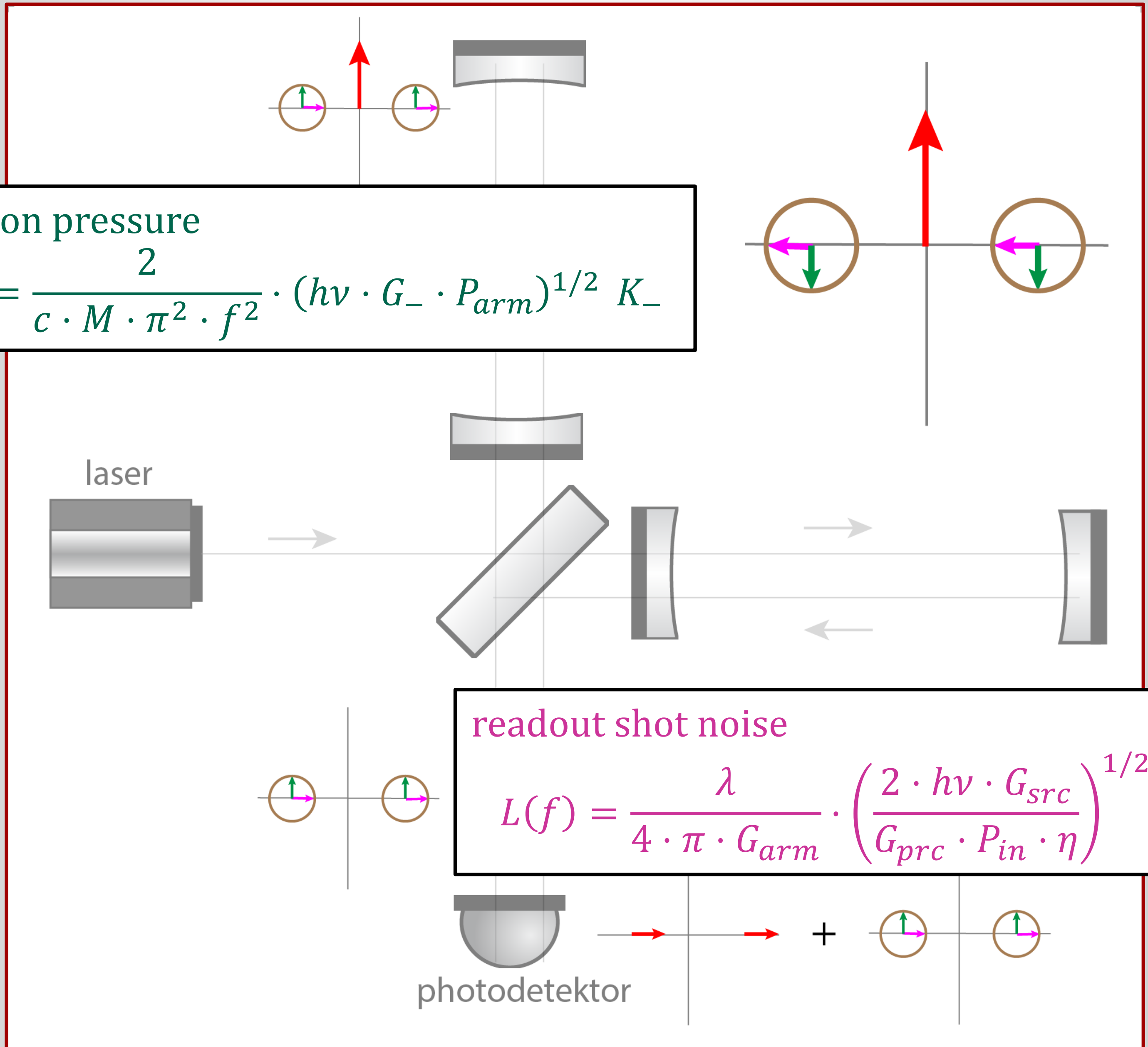

radiation pressure

$$L(f) = \frac{2}{c \cdot M \cdot \pi^2 \cdot f^2} \cdot (h\nu \cdot G_- \cdot P_{arm})^{1/2}\ K_-$$

readout shot noise

$$L(f) = \frac{\lambda}{4 \cdot \pi \cdot G_{arm}} \cdot \left(\frac{2 \cdot h\nu \cdot G_{src}}{G_{prc} \cdot P_{in} \cdot \eta}\right)^{1/2} \cdot \frac{1}{K_-}$$

Martynov D.V. et al., arXiv:1604.00439 [astro-ph.IM]

Quantum Vacuum Fluctuations – Radiation Pressure

radiation pressure

$$L(f) = \frac{2}{c \cdot M \cdot \pi^2 \cdot f^2} \cdot (h\nu \cdot G_- \cdot P_{arm})^{1/2}\ K_-$$

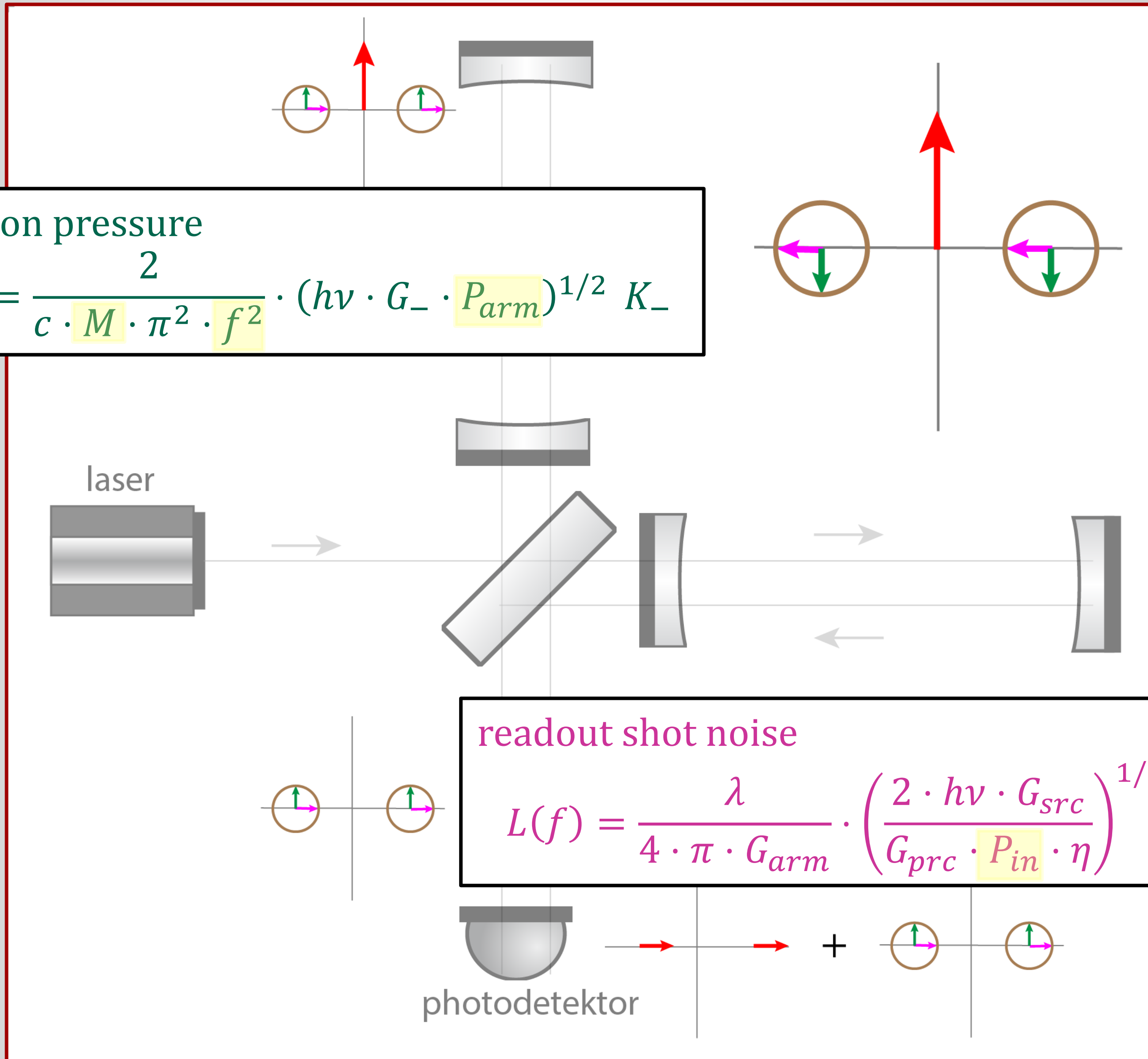

readout shot noise

$$L(f) = \frac{\lambda}{4 \cdot \pi \cdot G_{arm}} \cdot \left(\frac{2 \cdot h\nu \cdot G_{src}}{G_{prc} \cdot P_{in} \cdot \eta}\right)^{1/2} \cdot \frac{1}{K_-}$$

Martynov D.V. et al., arXiv:1604.00439 [astro-ph.IM]

Squeezing – Amplitued Quadrature

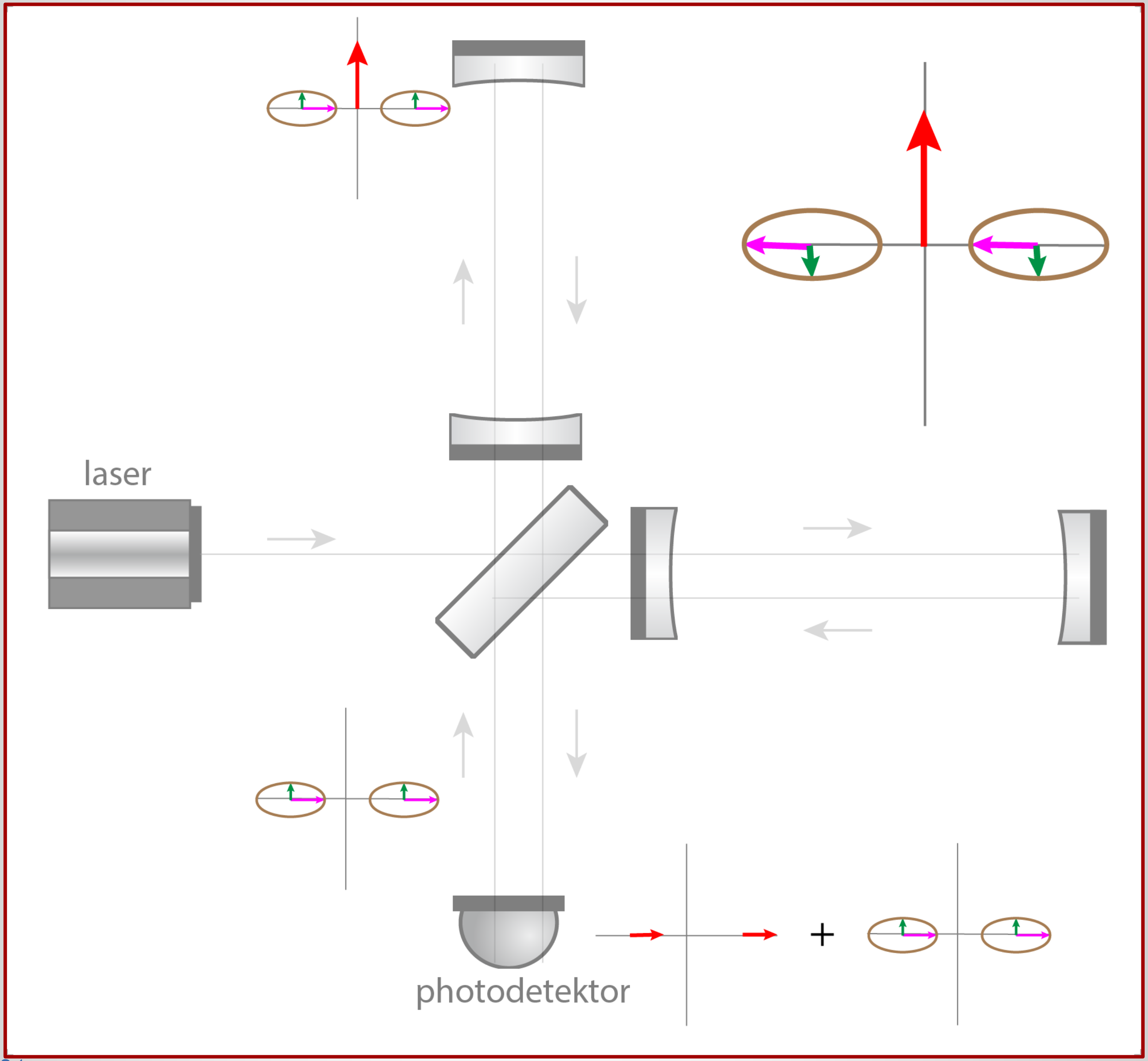

Leibniz Universität Hannover

Squeezing – Phase Quadrature

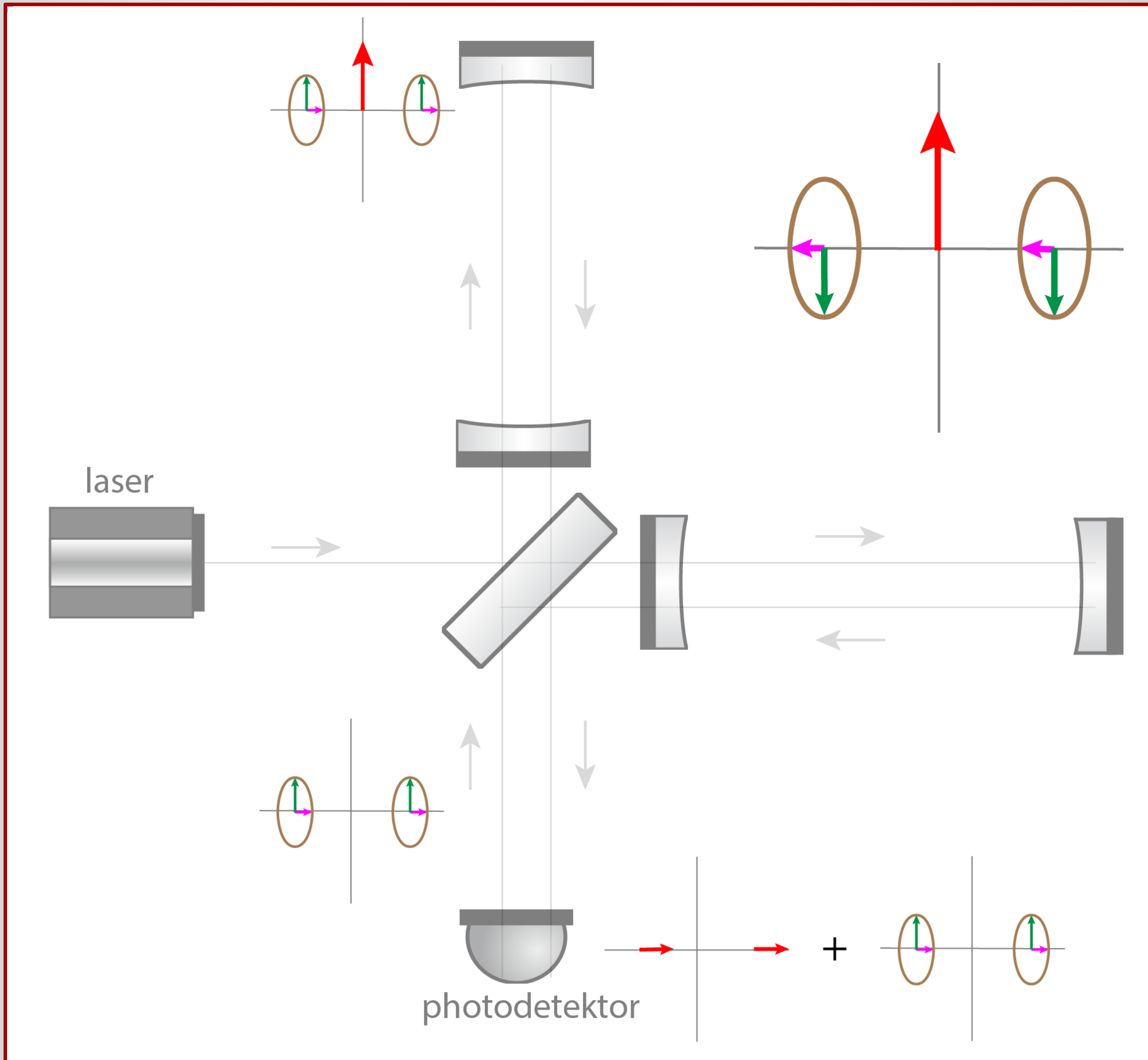

Signal Recycling

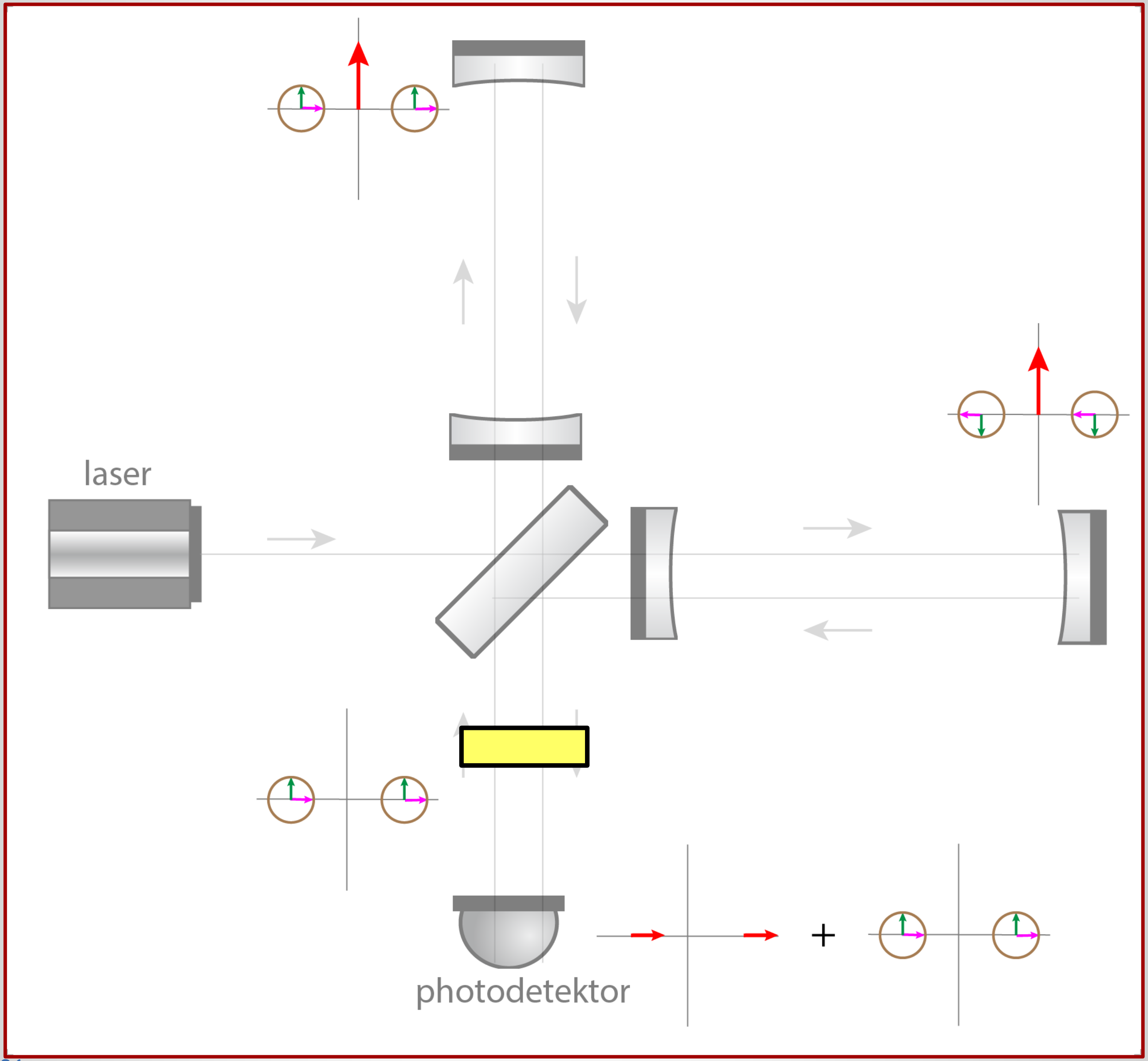

Advanced LIGO – Quantum Noise Shaping

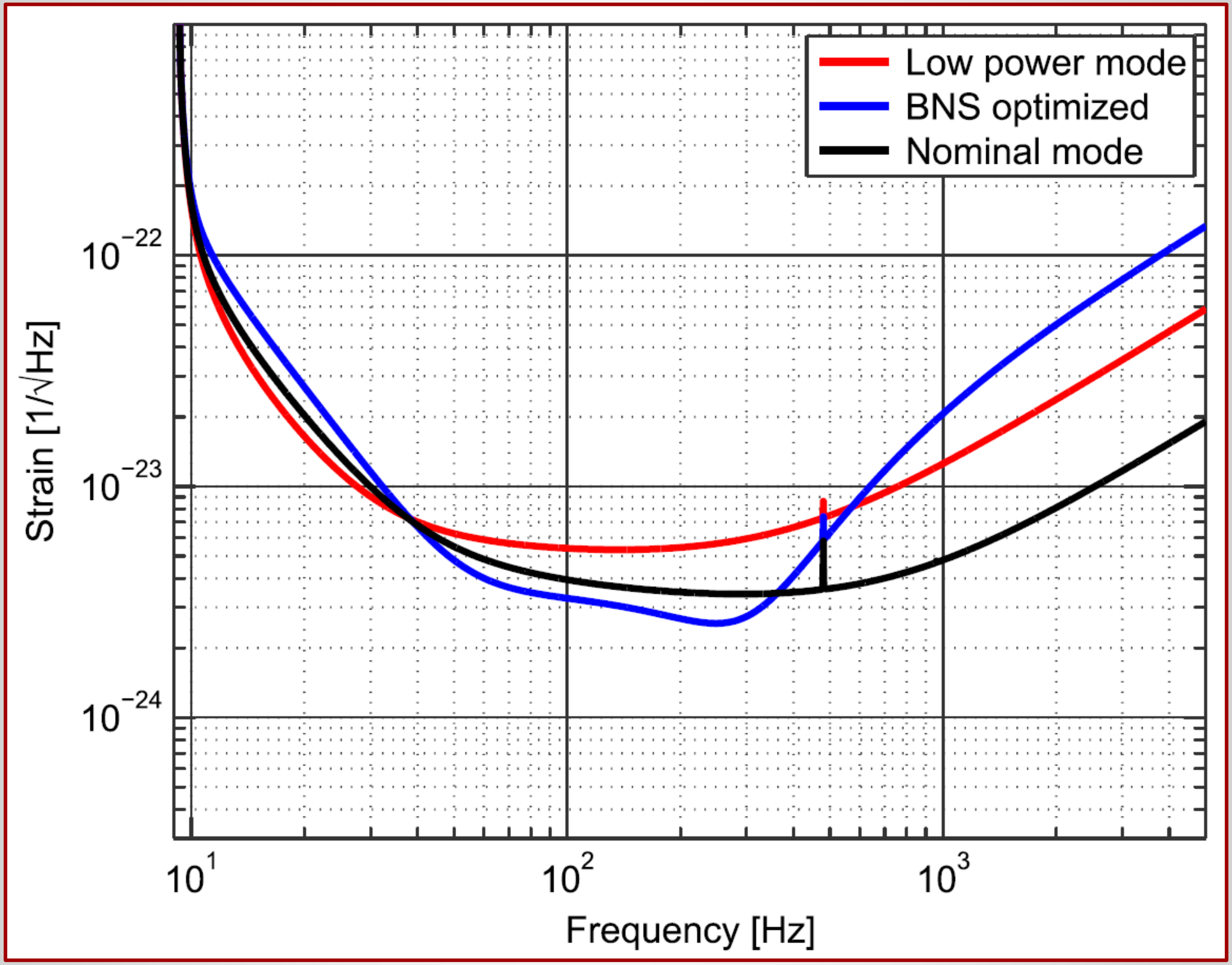

Aasi et al., Class. Quantum Grav. 32 (2015) 074001

Gravitational Wave Transducer

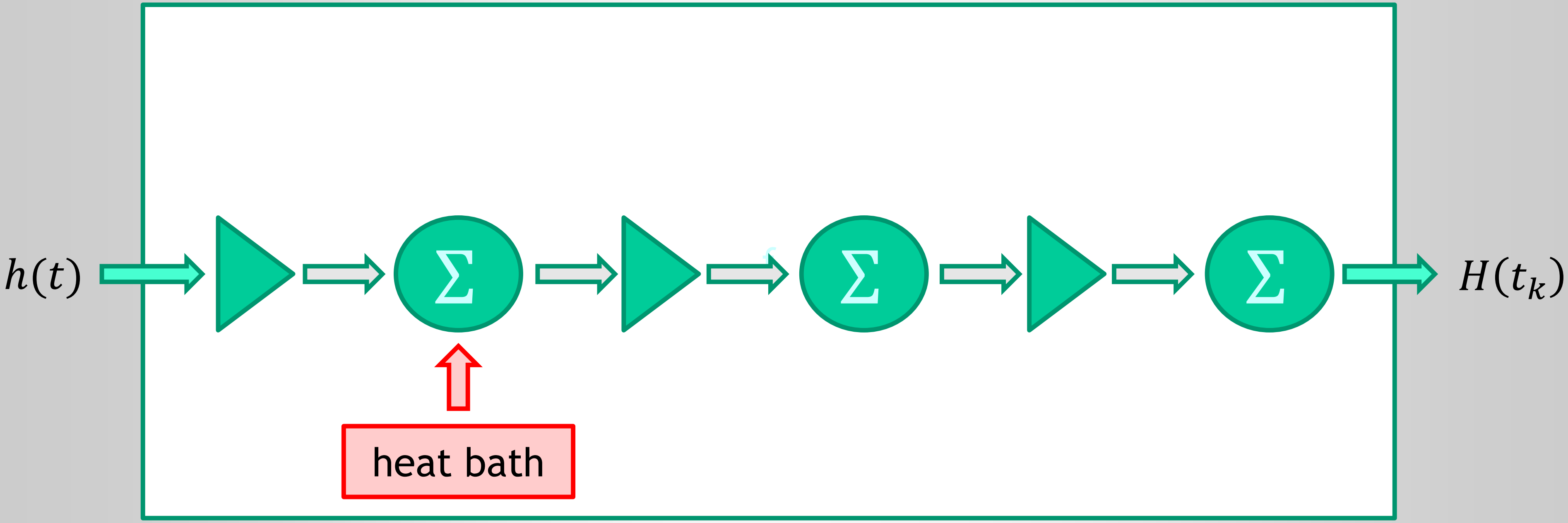

Leibniz Universität Hannover

Thermal Noise – Fluctuation Dissipation

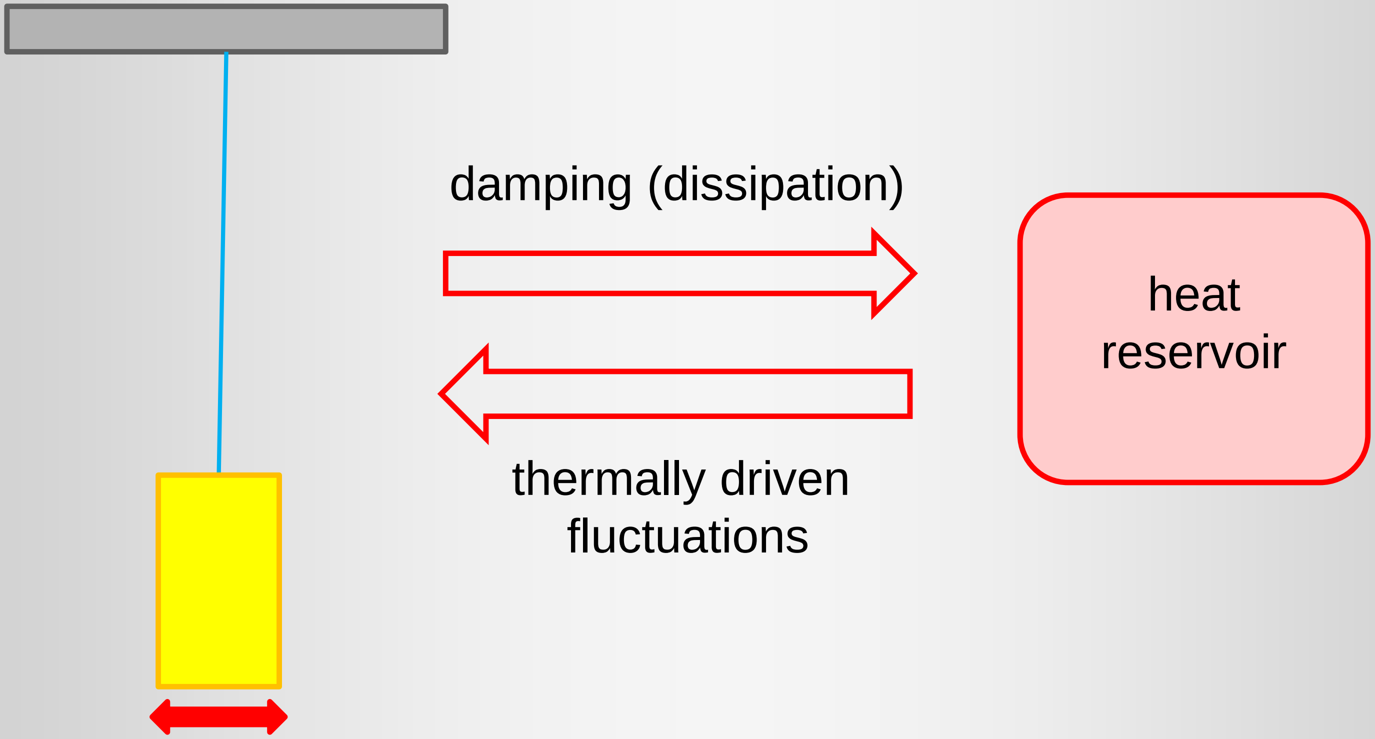

Thermal Noise – Fluctuation Dissipation

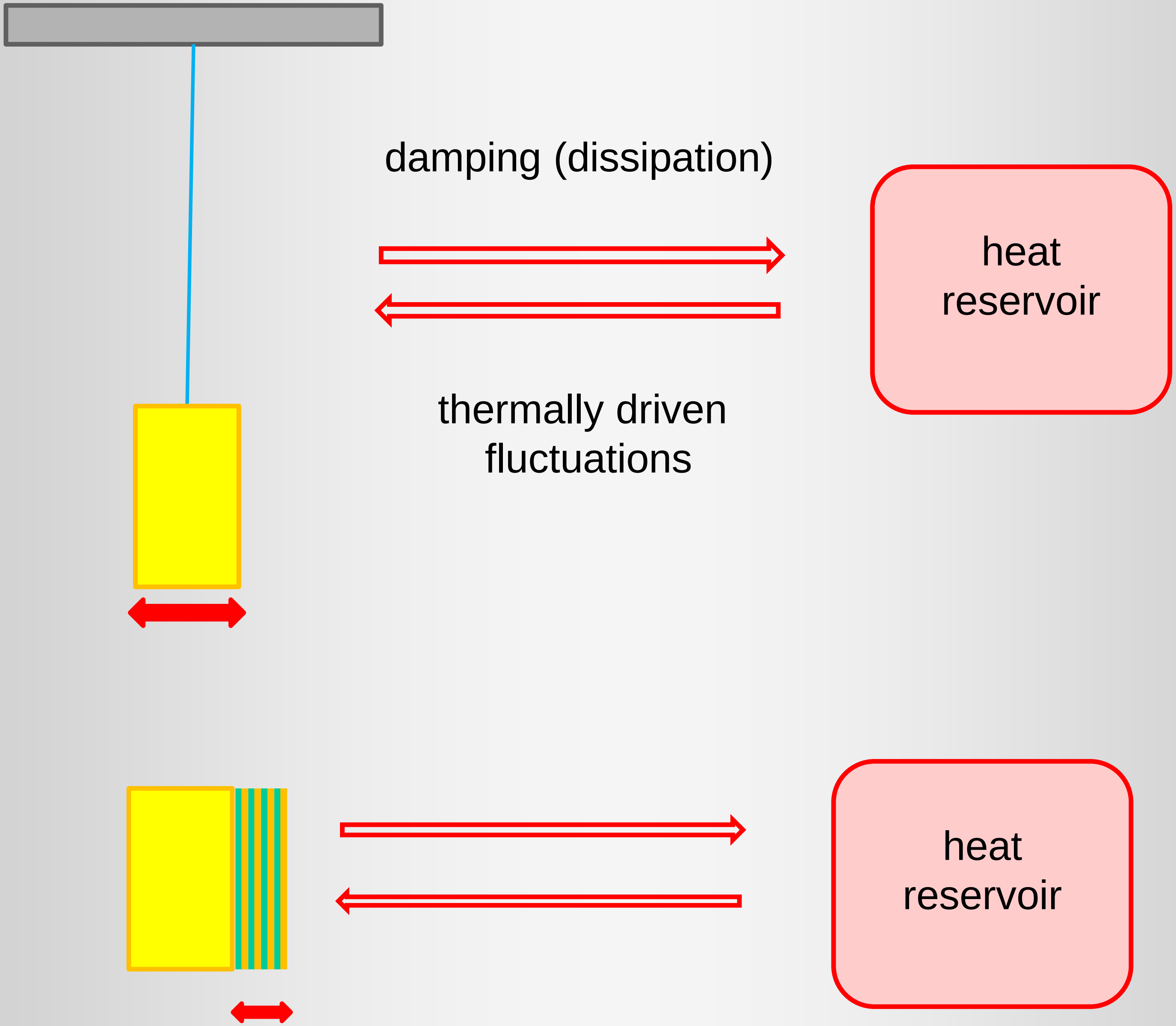

Gas and Squeezed Film

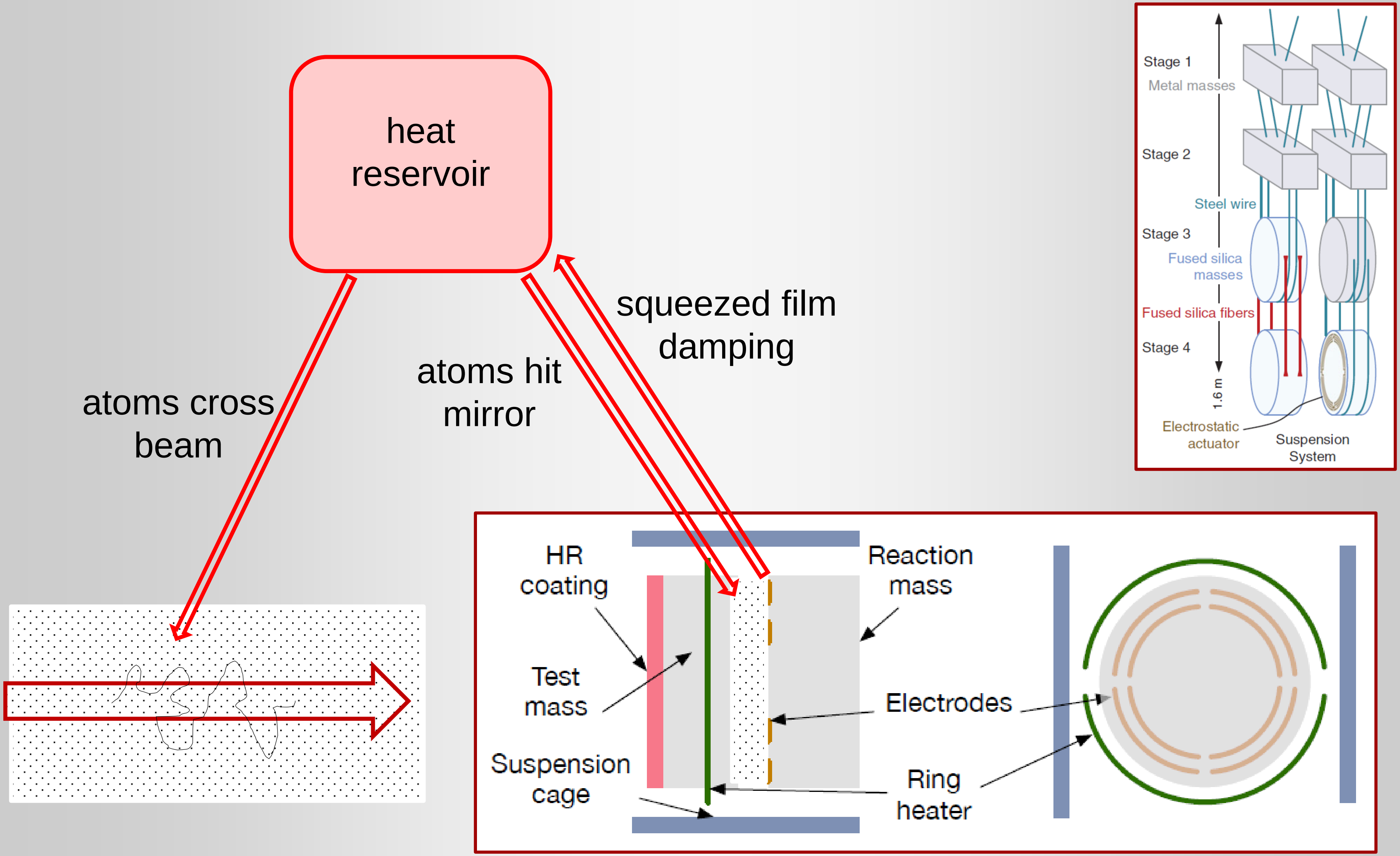

Martynov D.V. et al., arXiv:1604.00439 [astro-ph.IM]

Charge Noise

heat
reservoir

electrical potential
changes around
charged test mass

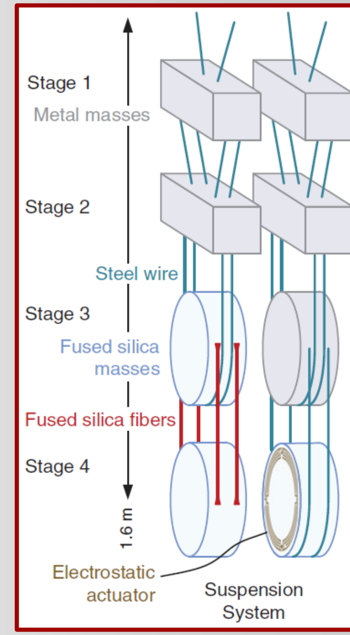

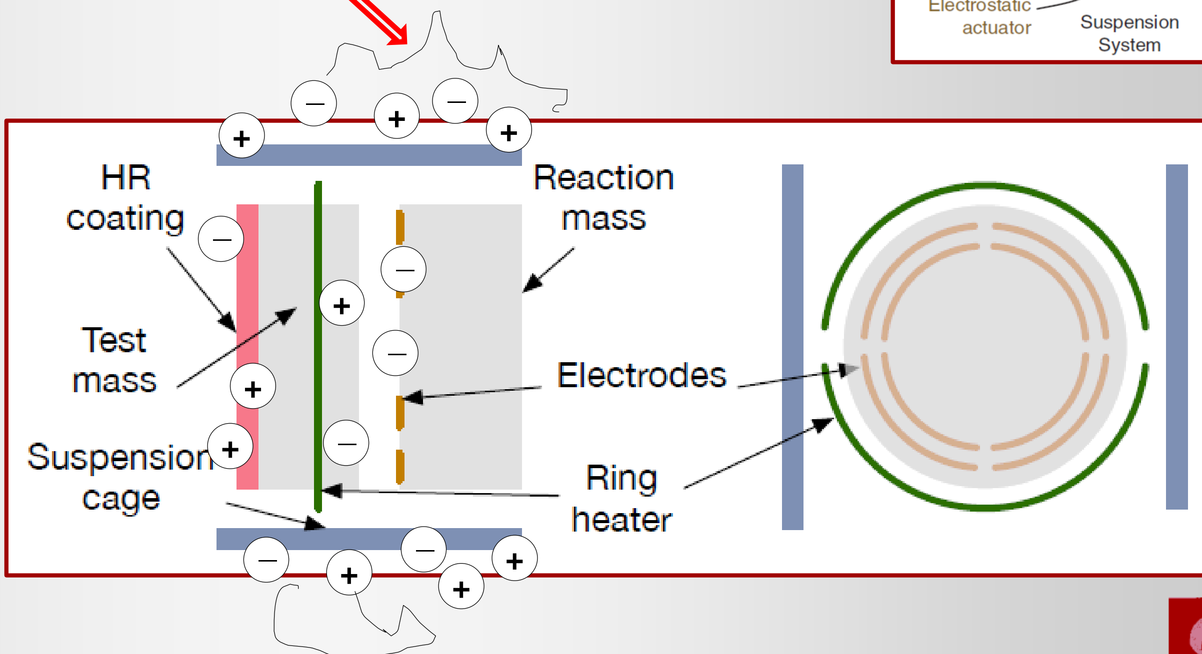

Martynov D.V. et al., arXiv:1604.00439 [astro-ph.IM]

Optical Layout Advanced LIGO (power levels O1)

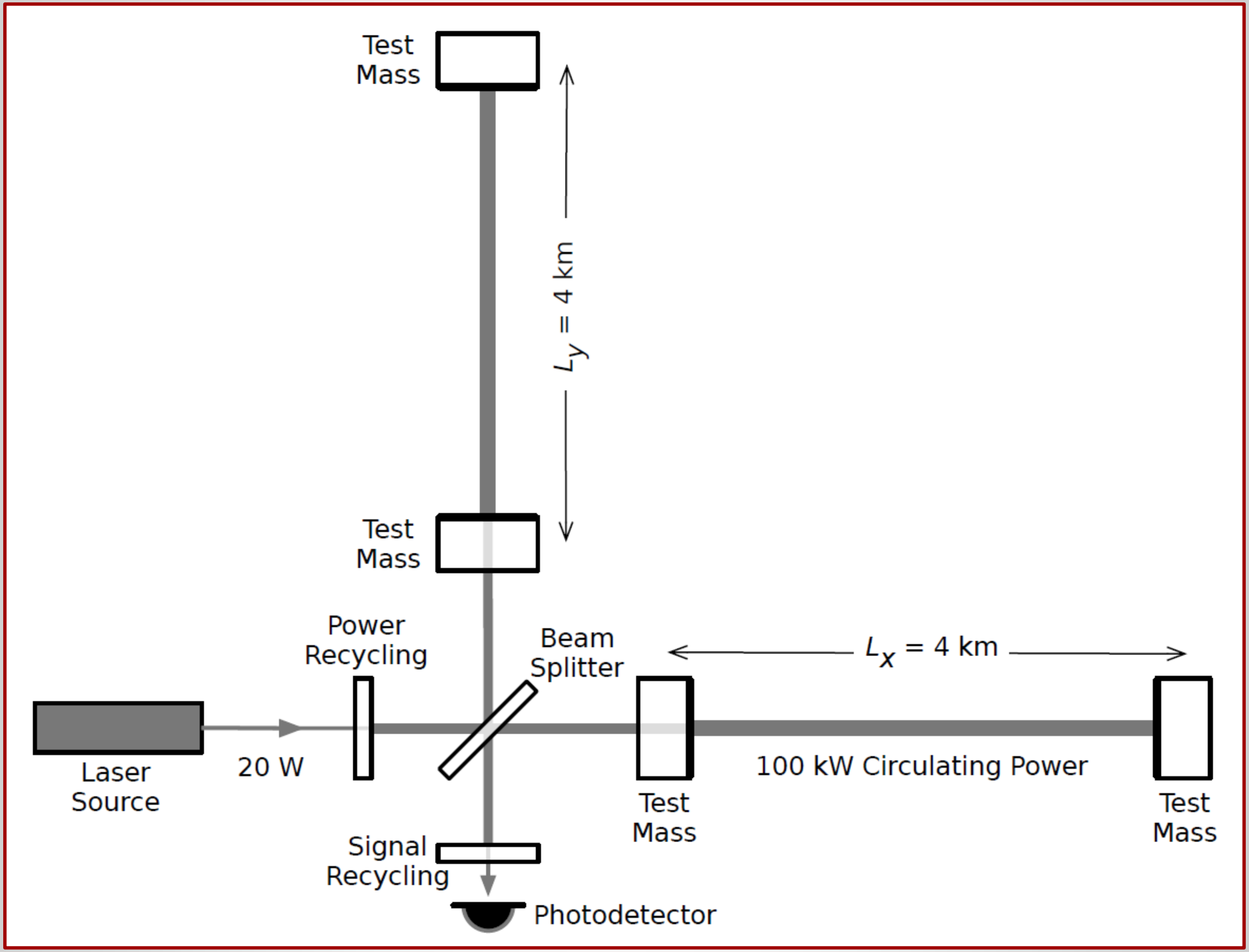

Phys. Rev. Lett. 116, 061102 (2016)

Advanced LIGO Laser

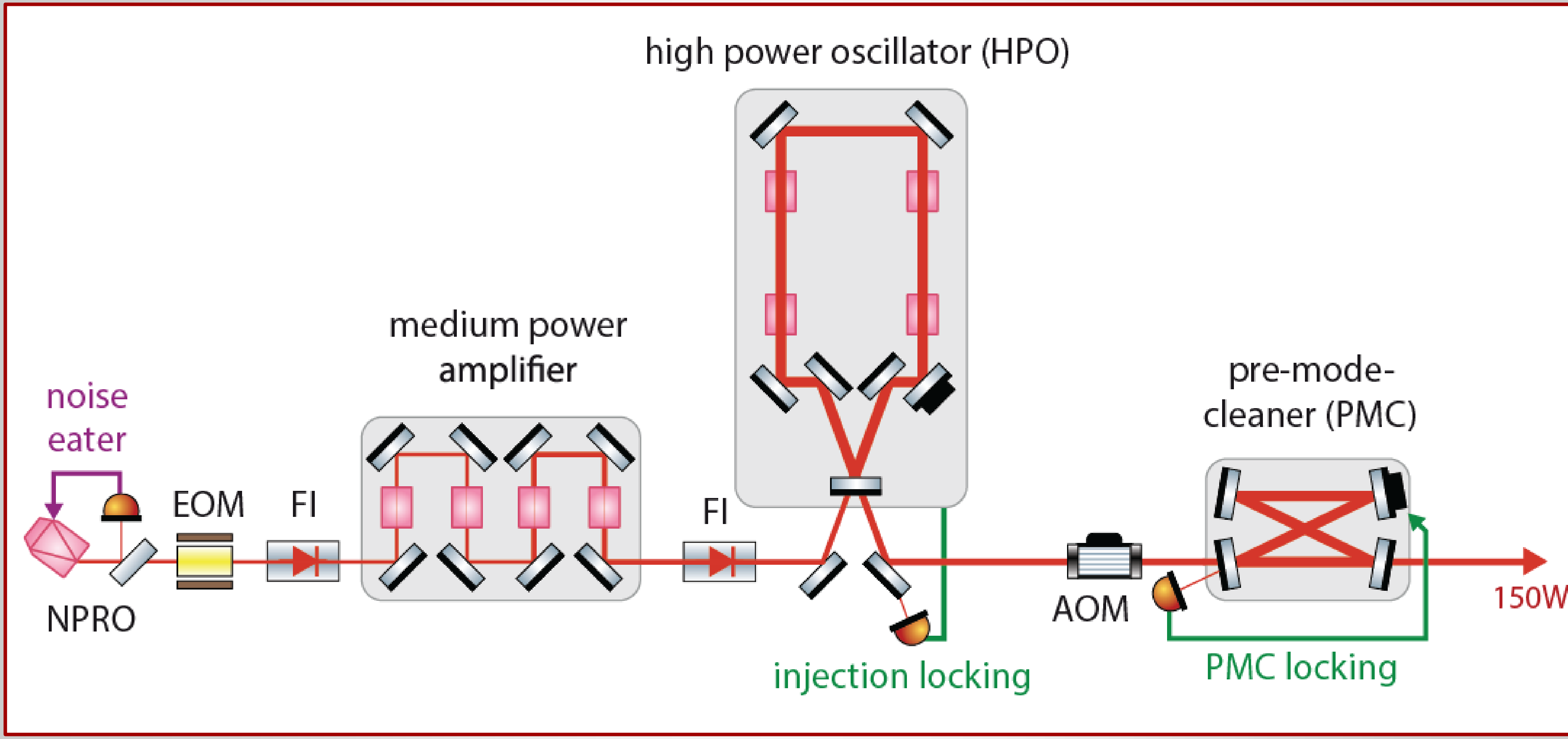

relative power noise: $RPN < 10^{-8}\ 1/\sqrt{Hz}$

relative frequency noise: $\frac{\Delta\nu}{\nu} < 10^{-17}\ Hz/\sqrt{Hz}$

power fraction in higher order spatial modes: HOM < 0,1%

beam pointing at 4km: $\delta x \ < 0{,}2\ mm$

Kwee et al. Opt. Lett. (2009), Kwee et al. Opt. Express (2012)

Advanced LIGO Laser Beam Preparation

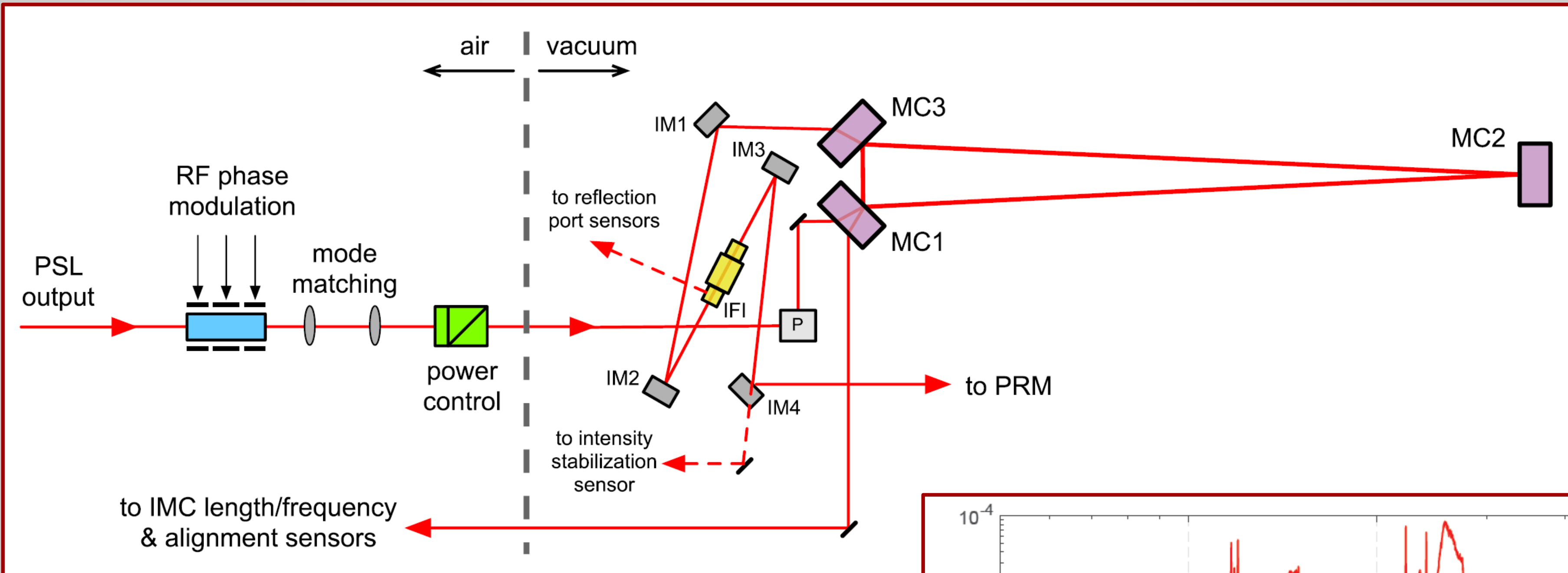

input mode clearer
- length: 32.9m (round trip)
- finesse: 500
- beam jitter filtering: ≈ 150

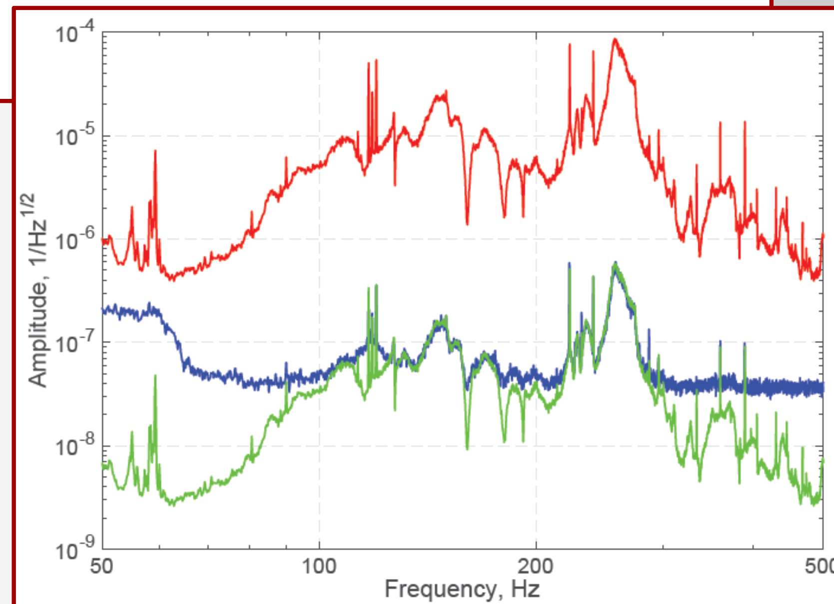

Aasi et al., Class. Quantum Grav. 32 (2015) 074001 ; Martynov D.V. et al arXiv:1604.00439 [astro-ph.IM]

Vacuum System

Leibniz
Universität
Hannover

Seismic Isolation System

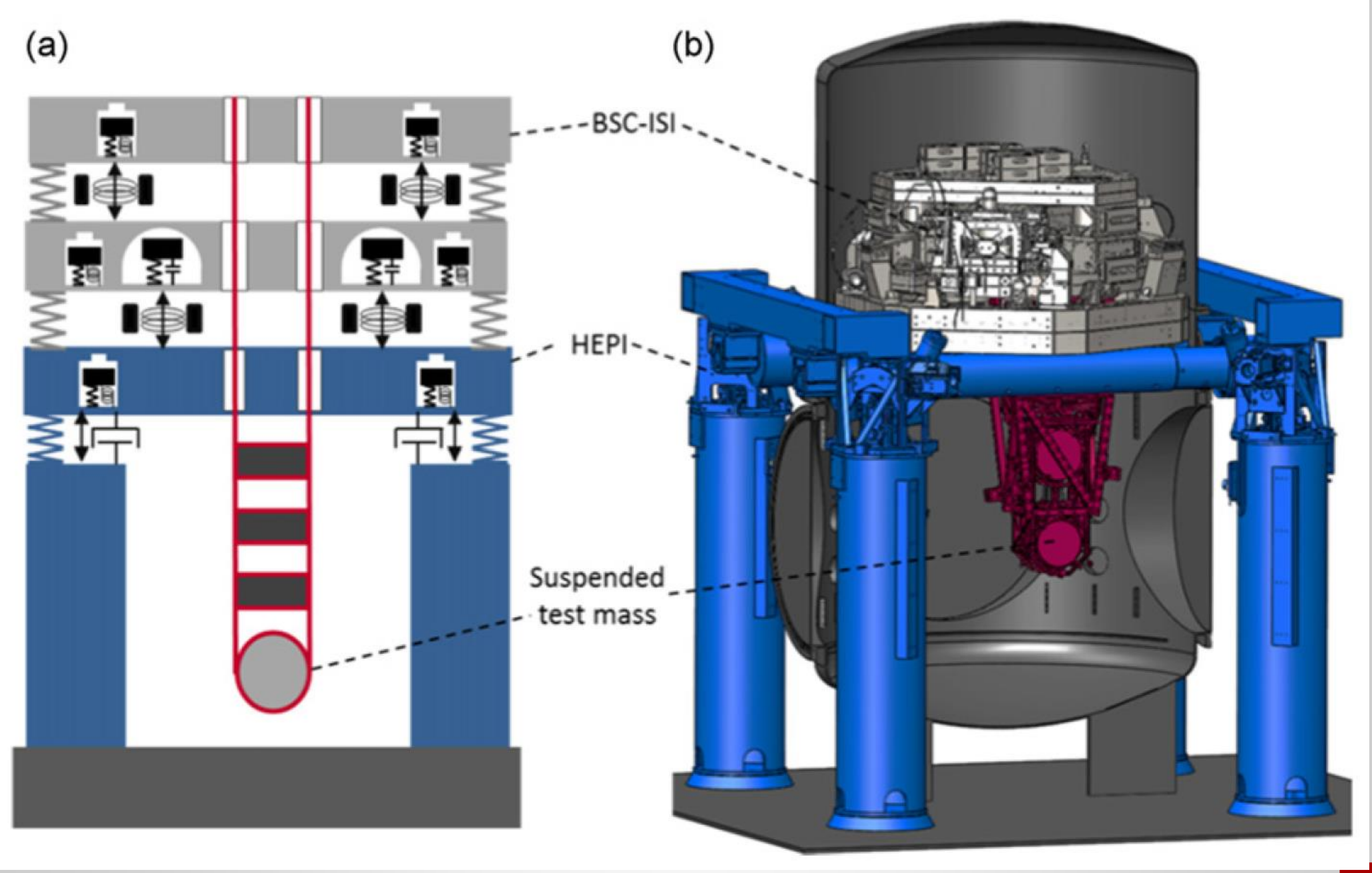

Matichard F. et al., Class. Quantum Grav. 32 (2015) 185003

Test Mass – Seismic Isolation

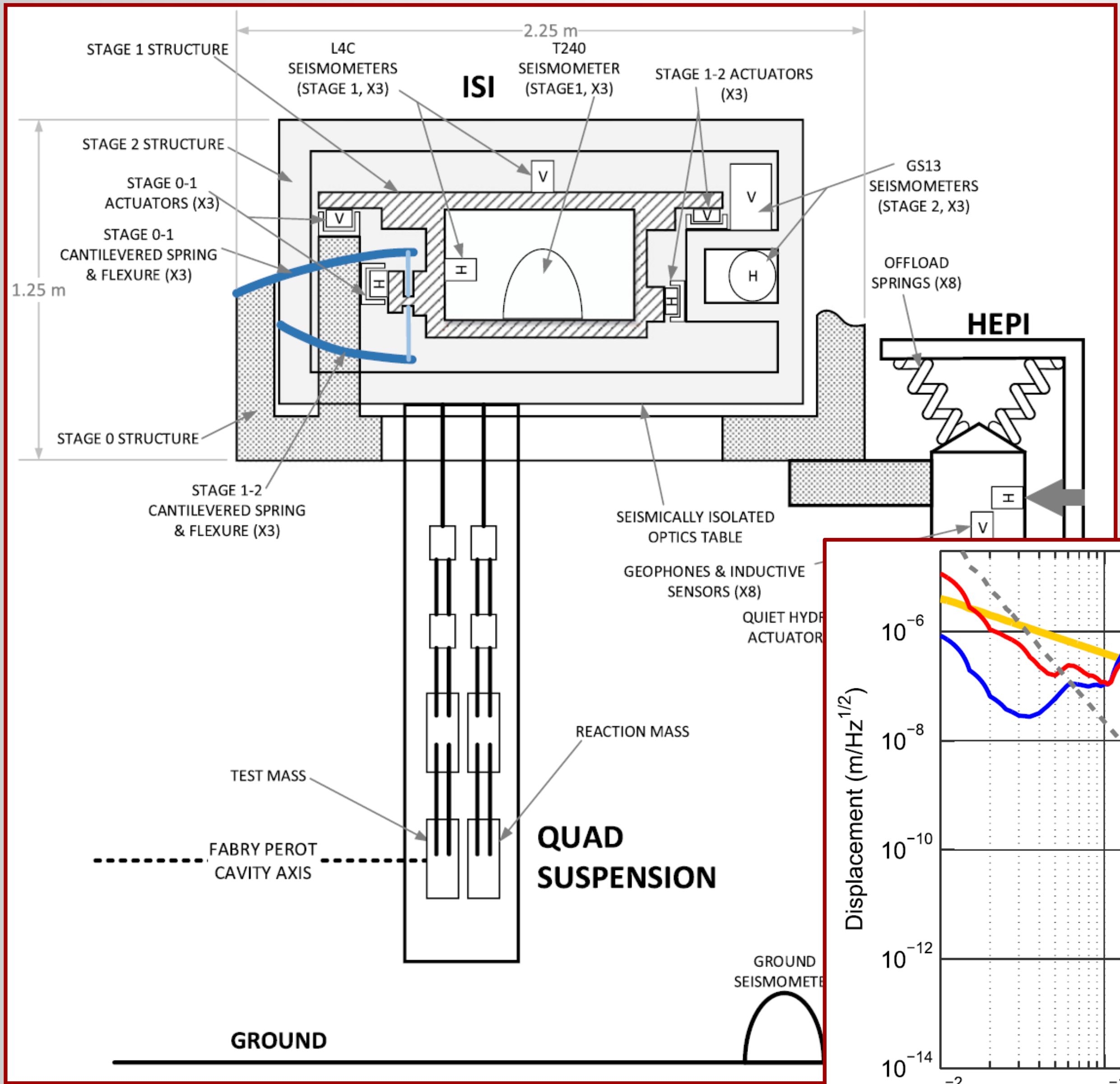

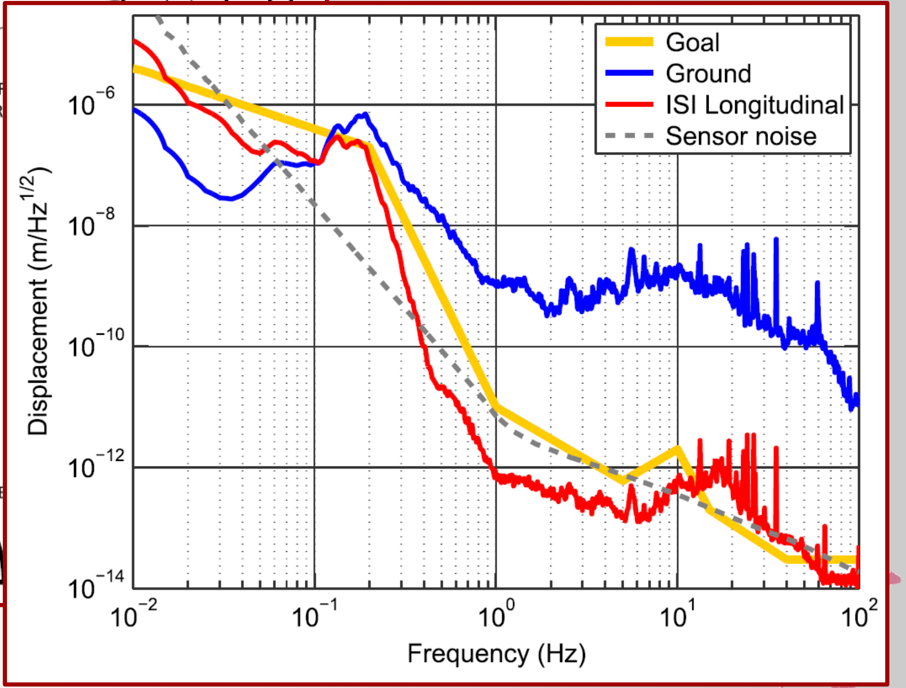

Aasi et al., Class. Quantum Grav. 32 (2015) 074001

Advanced LIGO seismic isolation system

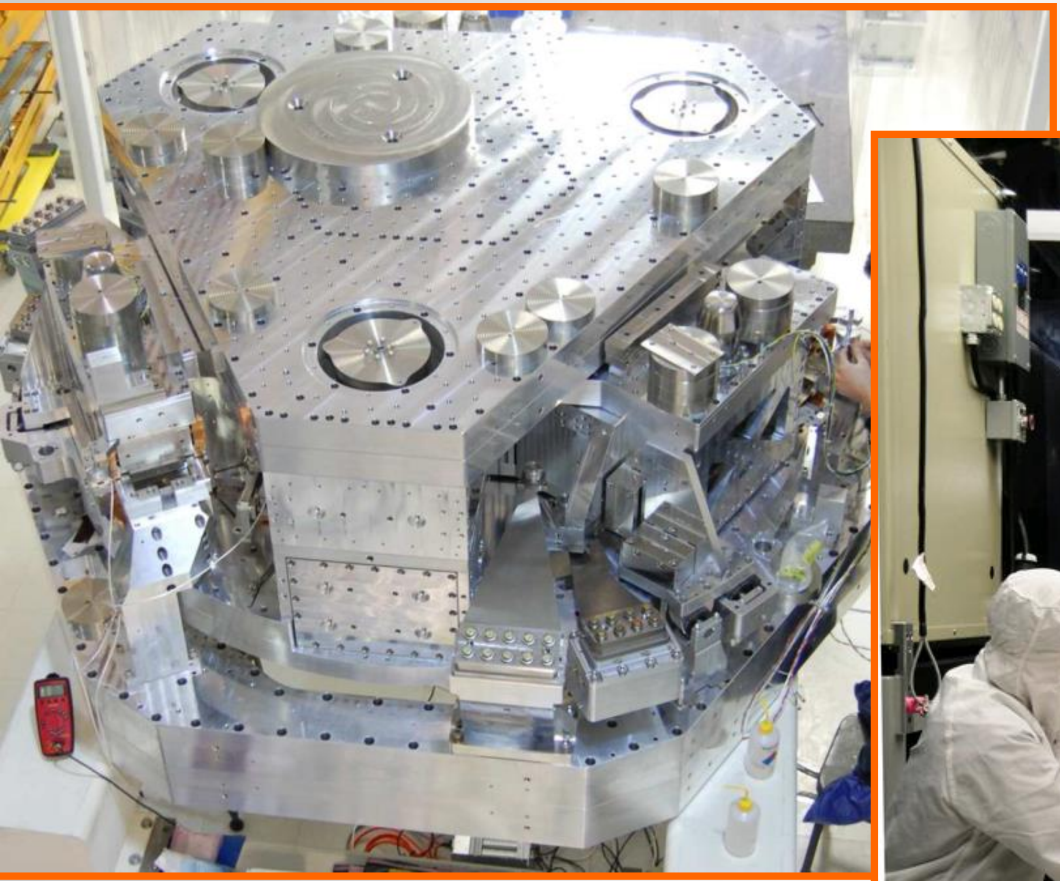

Low Loss Quadruple Pendulum Suspension

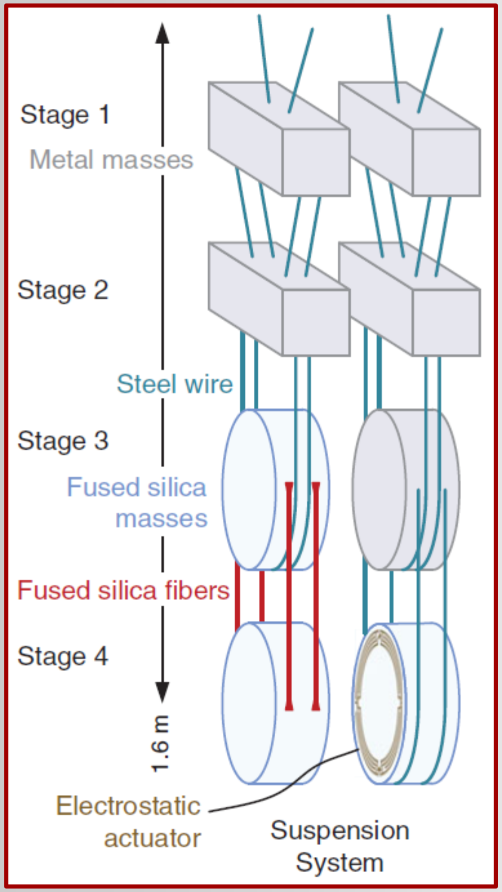

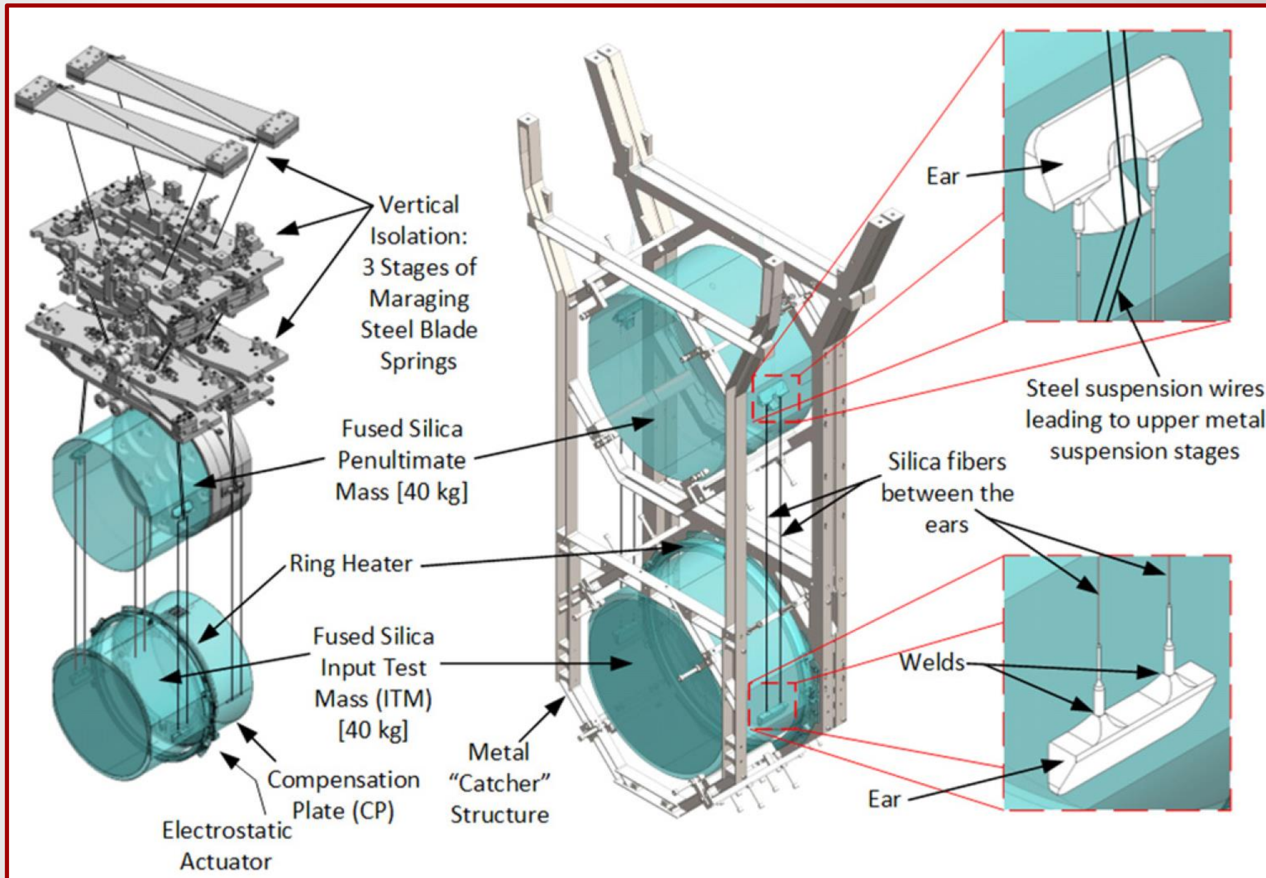

Abbott et al. PRL 116, 131103 (2016); Aasi et al., Class. Quant. Grav. 32 (2015) 074001; Martynov D.V. et al arXiv:1604.00439

Mirrors

	Surface error, central 160 mm diam., power and astigmatism removed, rms		
	$> 1\ \mathrm{mm}^{-1}$	$1\text{–}750\ \mathrm{mm}^{-1}$	Radius of curvature spread
Specification	< 0.3 nm	< 0.16 nm	−5, +10 m
Actual	0.08–0.23 nm	0.07–0.14 nm	−1.5, +1 m

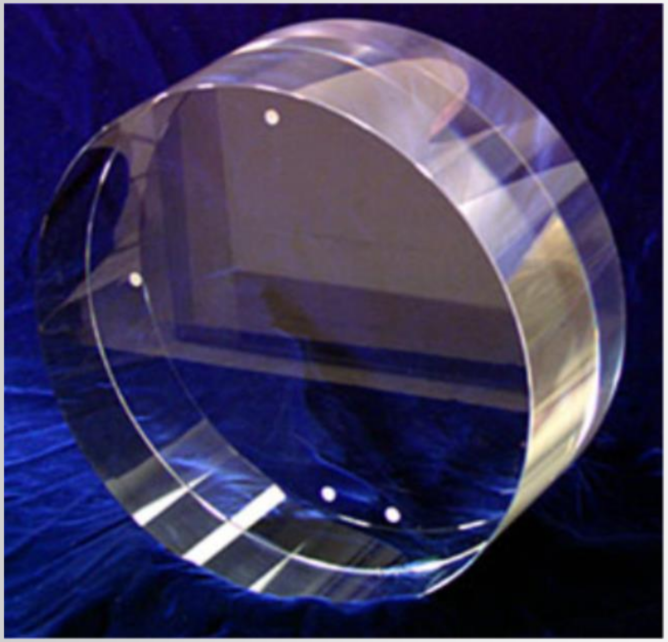

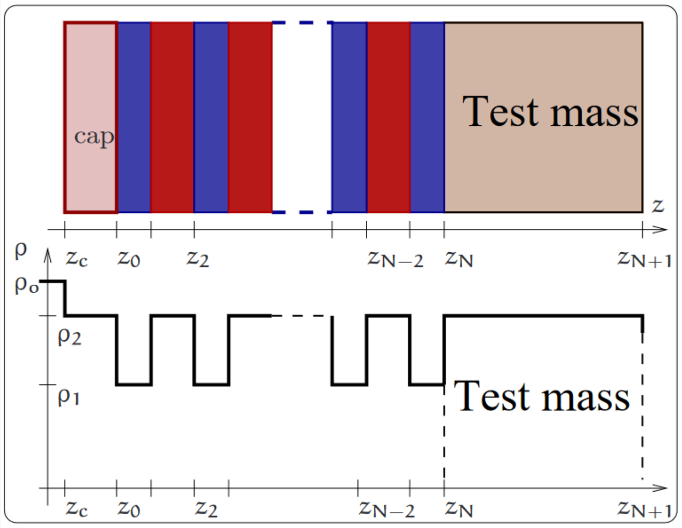

25% Ti doping of the TaO_5 stacks
=> 40% mechanical loss reduction

Aasi et al., Class. Quantum Grav. 32 (2015) 074001 ; arXiv:1005.3138 [gr-qc]

Armlength Stabilization System

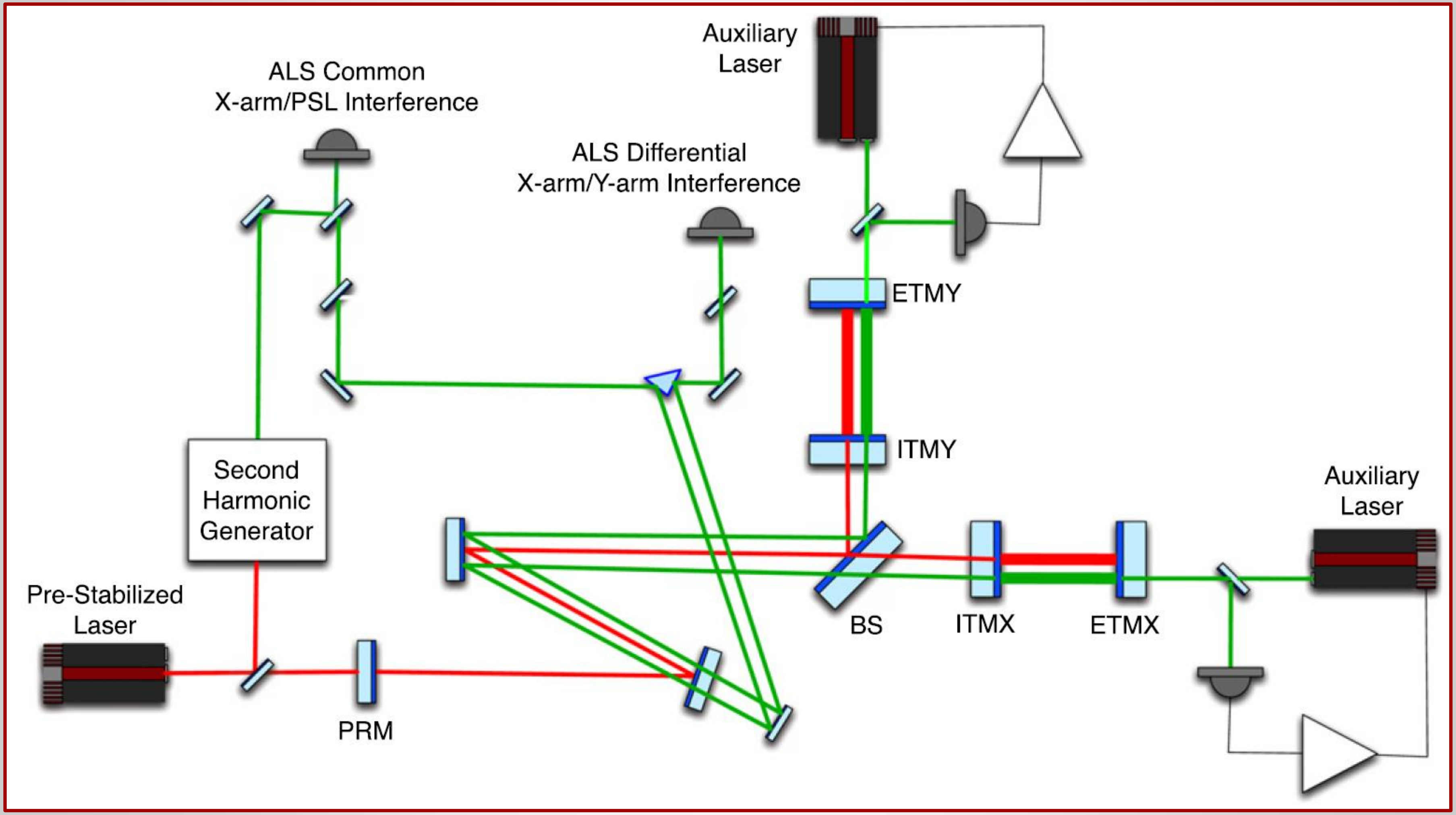

Aasi et al., Class. Quantum Grav. 32 (2015) 074001

Thermal Compensation System

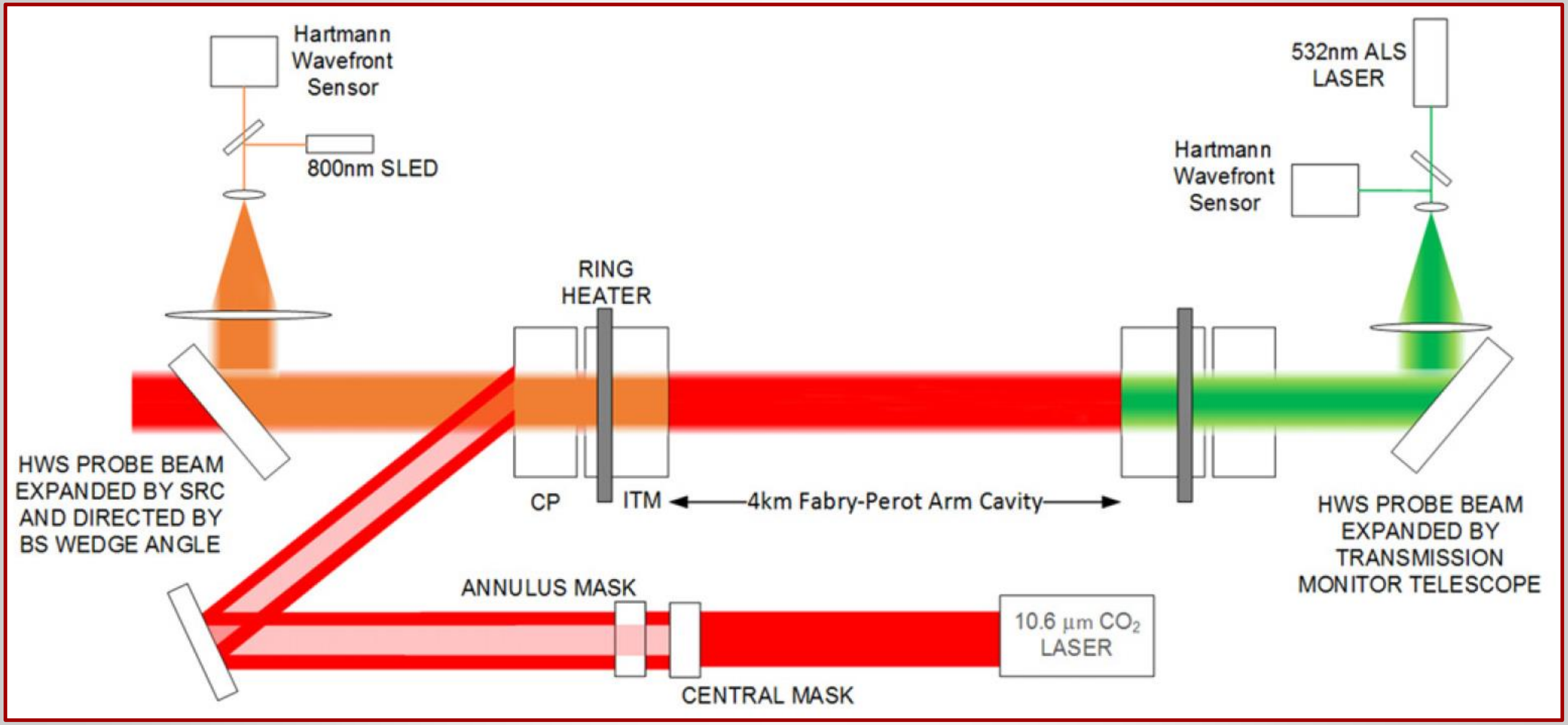

Aasi et al., Class. Quantum Grav. 32 (2015) 074001

Length Sensing and Control

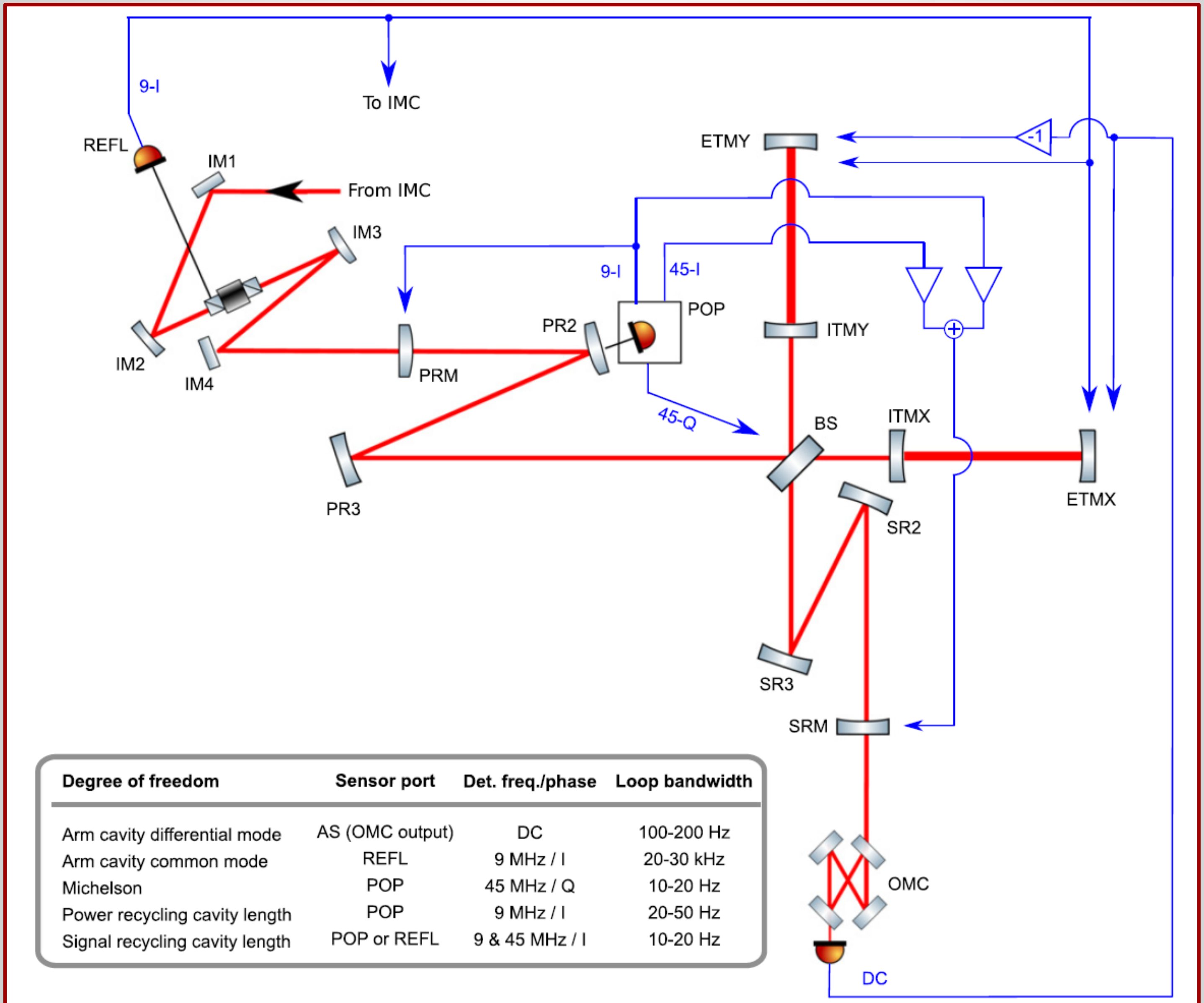

Degree of freedom	Sensor port	Det. freq./phase	Loop bandwidth
Arm cavity differential mode	AS (OMC output)	DC	100-200 Hz
Arm cavity common mode	REFL	9 MHz / I	20-30 kHz
Michelson	POP	45 MHz / Q	10-20 Hz
Power recycling cavity length	POP	9 MHz / I	20-50 Hz
Signal recycling cavity length	POP or REFL	9 & 45 MHz / I	10-20 Hz

Aasi et al., Class. Quantum Grav. 32 (2015) 074001

Calibration via Radiation Pressure

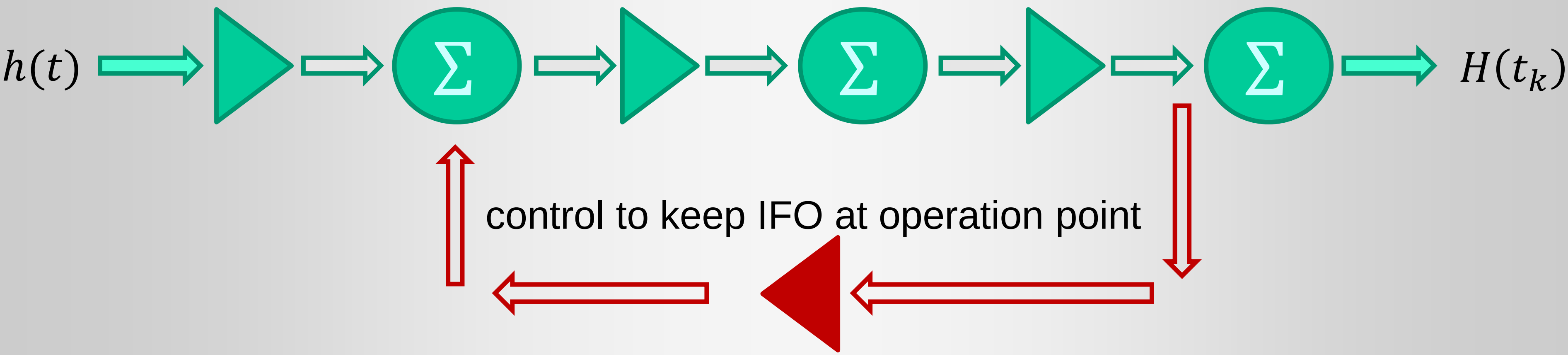

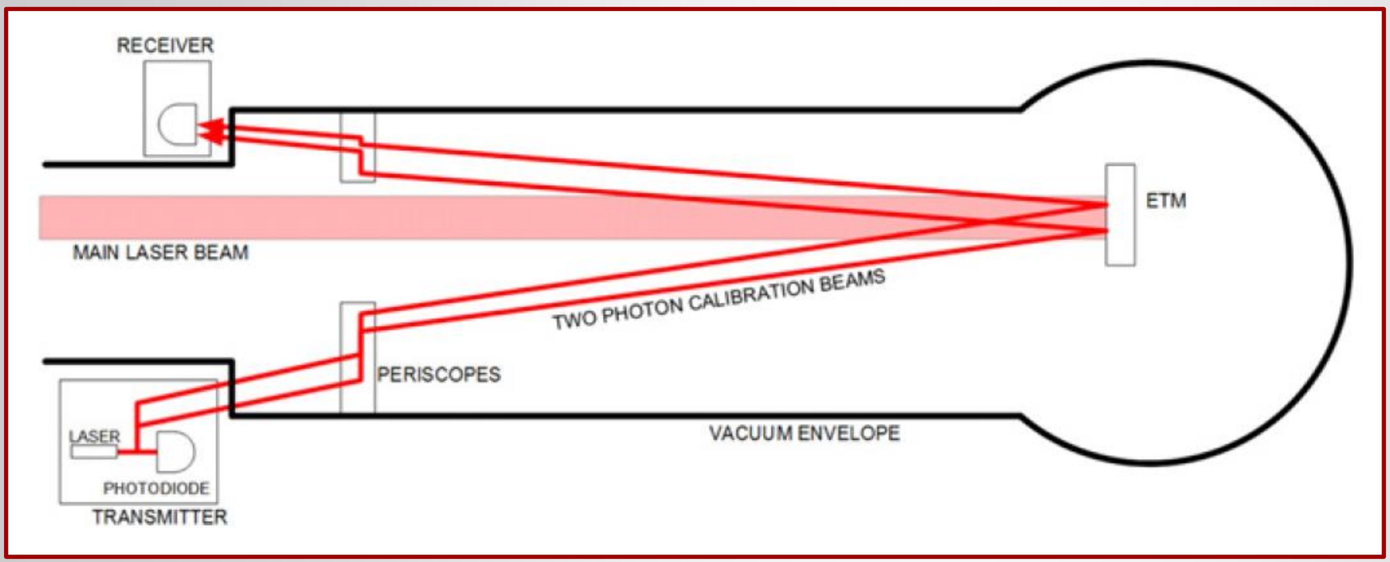

uncertainties:

- phase: 10 deg
- amplitude: 10%

Advanced LIGO

Parameter	*Initial LIGO*	*Advanced LIGO*
Input Laser Power	10 W (10 kW arm)	180 W (>700 kW arm)
Mirror Mass	10 kg	40 kg
Interferometer Topology	Power-recycled Fabry-Perot arm cavity Michelson	Dual-recycled Fabry-Perot arm cavity Michelson (stable RC)
GW Readout Method	RF heterodyne	DC homodyne
Optimal Strain Sensitivity	3×10^{-23} / rHz	Tunable, better than 5×10^{-24} / rHz in broadband
Seismic Isolation Performance	f_{low} ~ 50 Hz	f_{low} ~ 12 Hz
Mirror Suspensions	Single Pendulum	Quadruple pendulum

Sensitivity Improvement Advanced LIGO

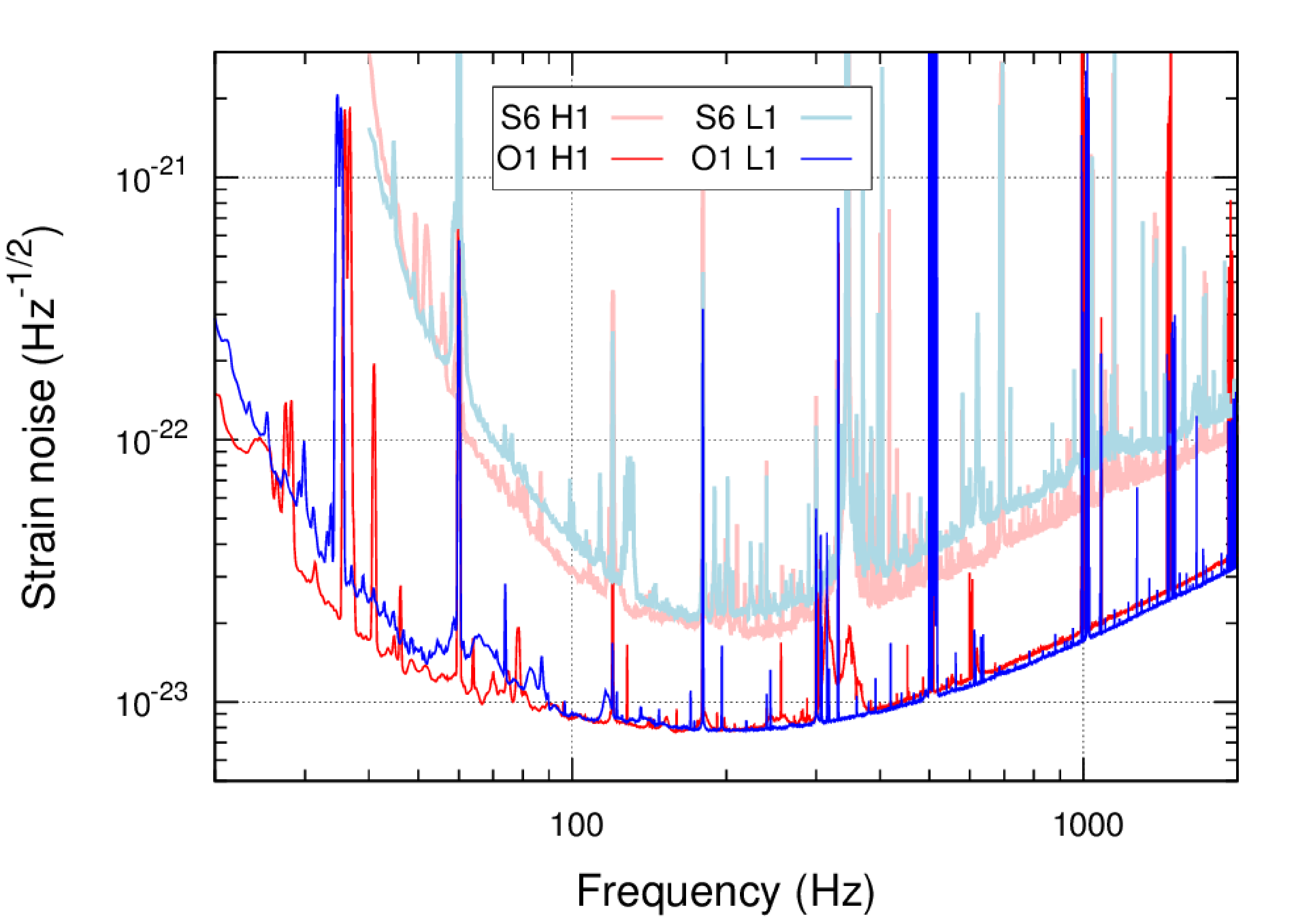

Noise Morphology During O1

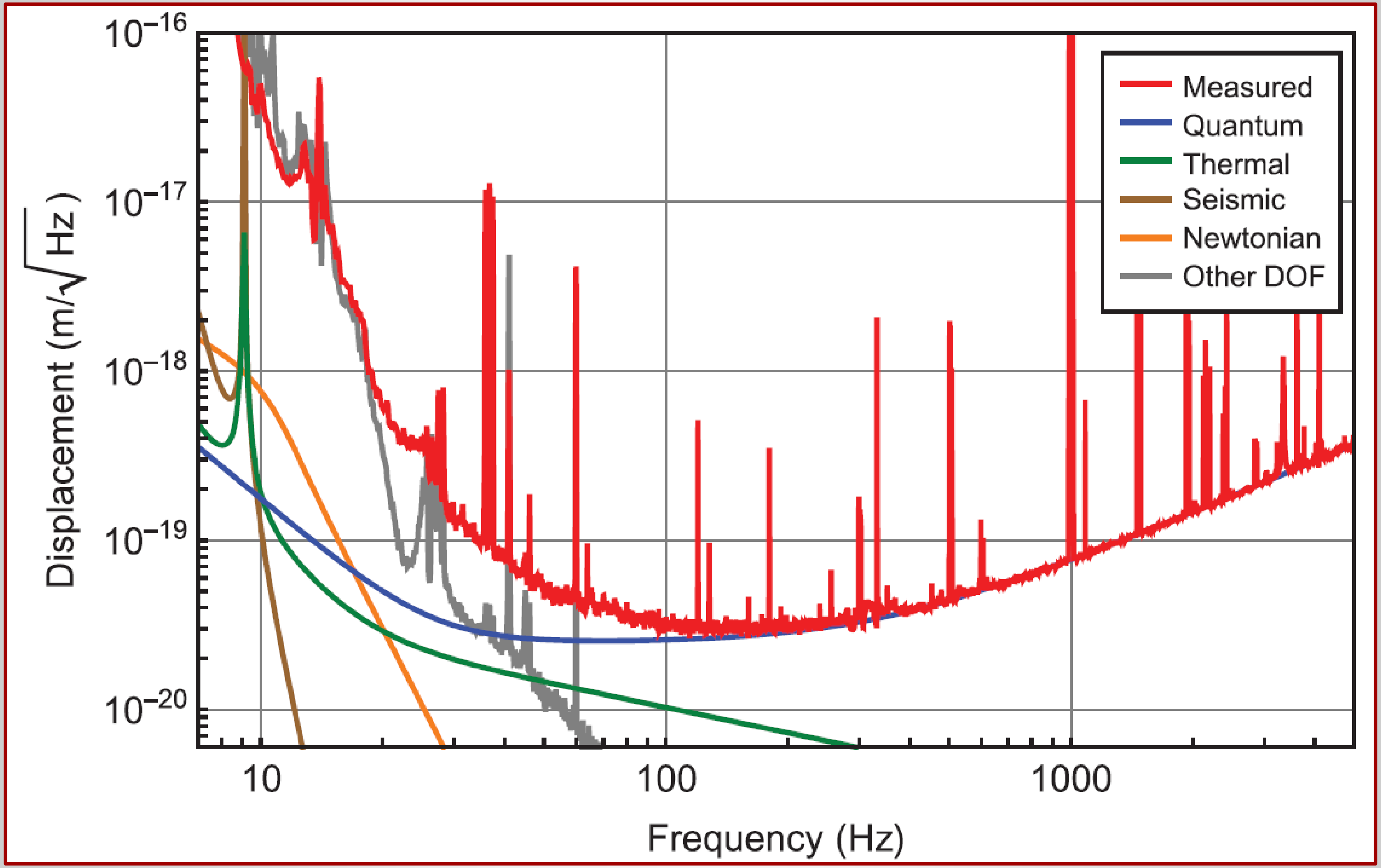

Abbott et al. PRL 116, 131103 (2016)

Noise Projections – High Frequencies

$$L_{noise}(f) \equiv L_0 \cdot h_{noise}(f) = T(f) \cdot N(f)$$

via signal injection

via independent (witness) sensor

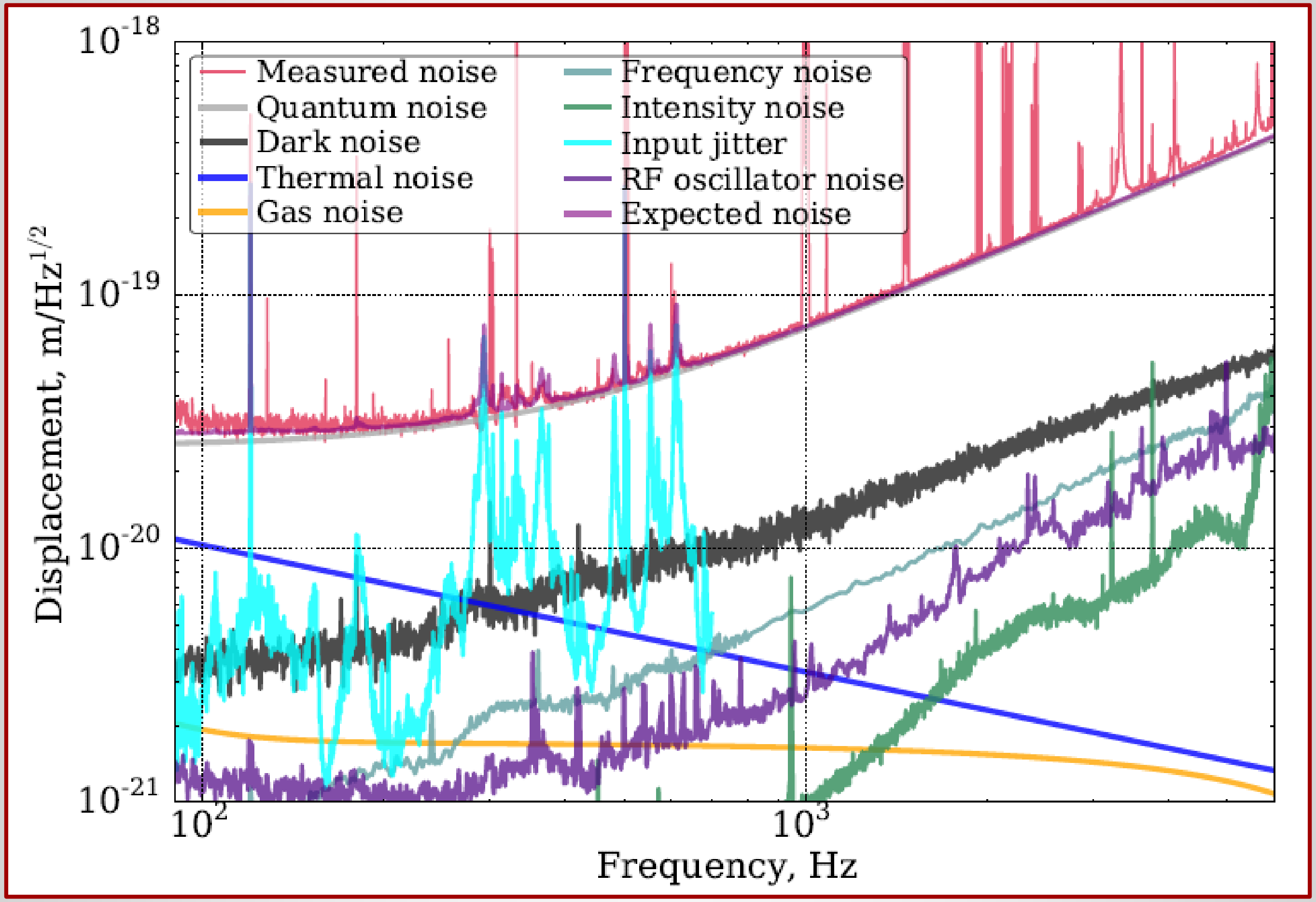

Martynov D.V. et al ,arXiv:1604.00439 [astro-ph.IM]

Noise Projections – Low Frequencies

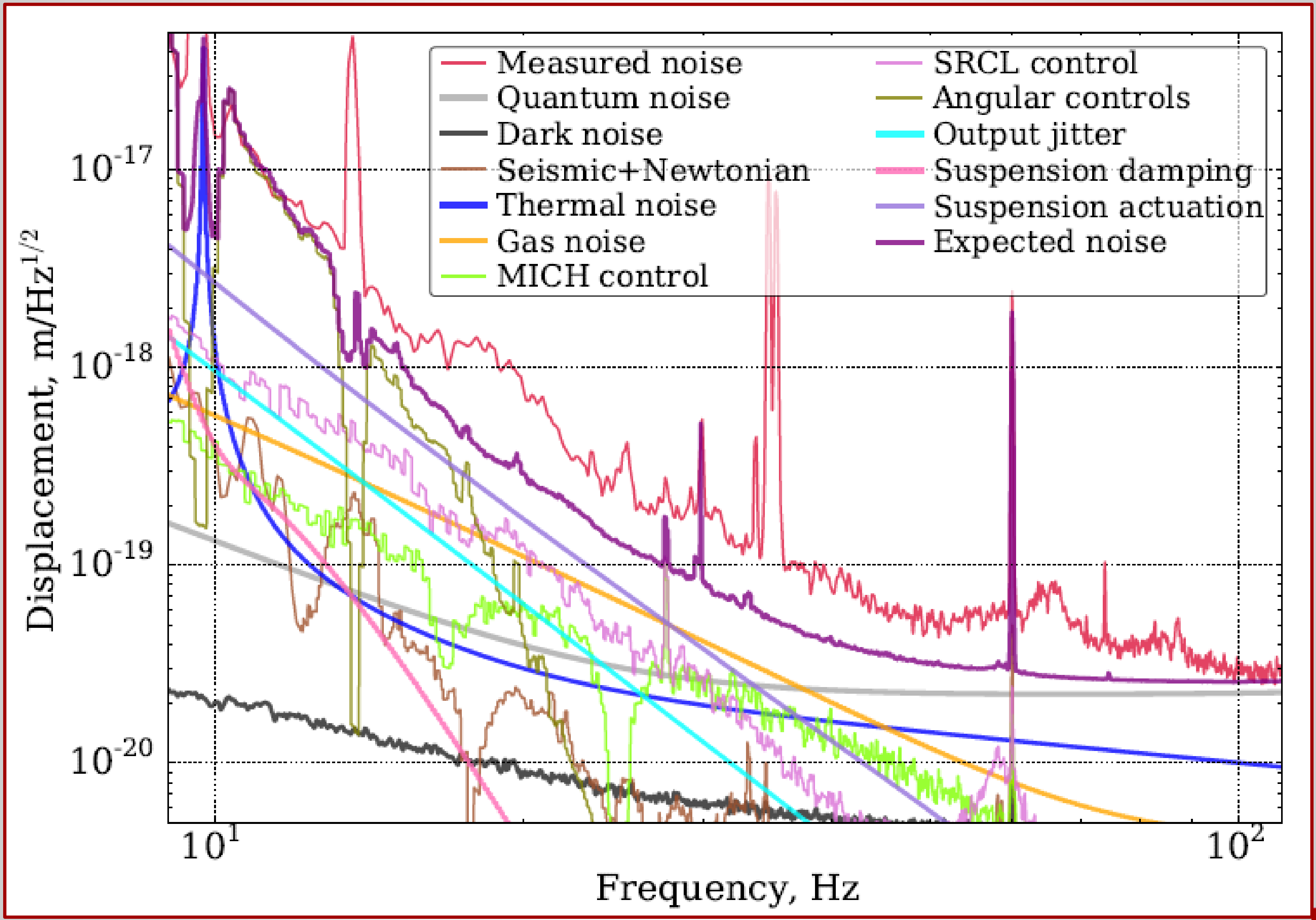

Martynov D.V. et al ,arXiv:1604.00439 [astro-ph.IM]

Time Varying Response and Stationarity (O1)

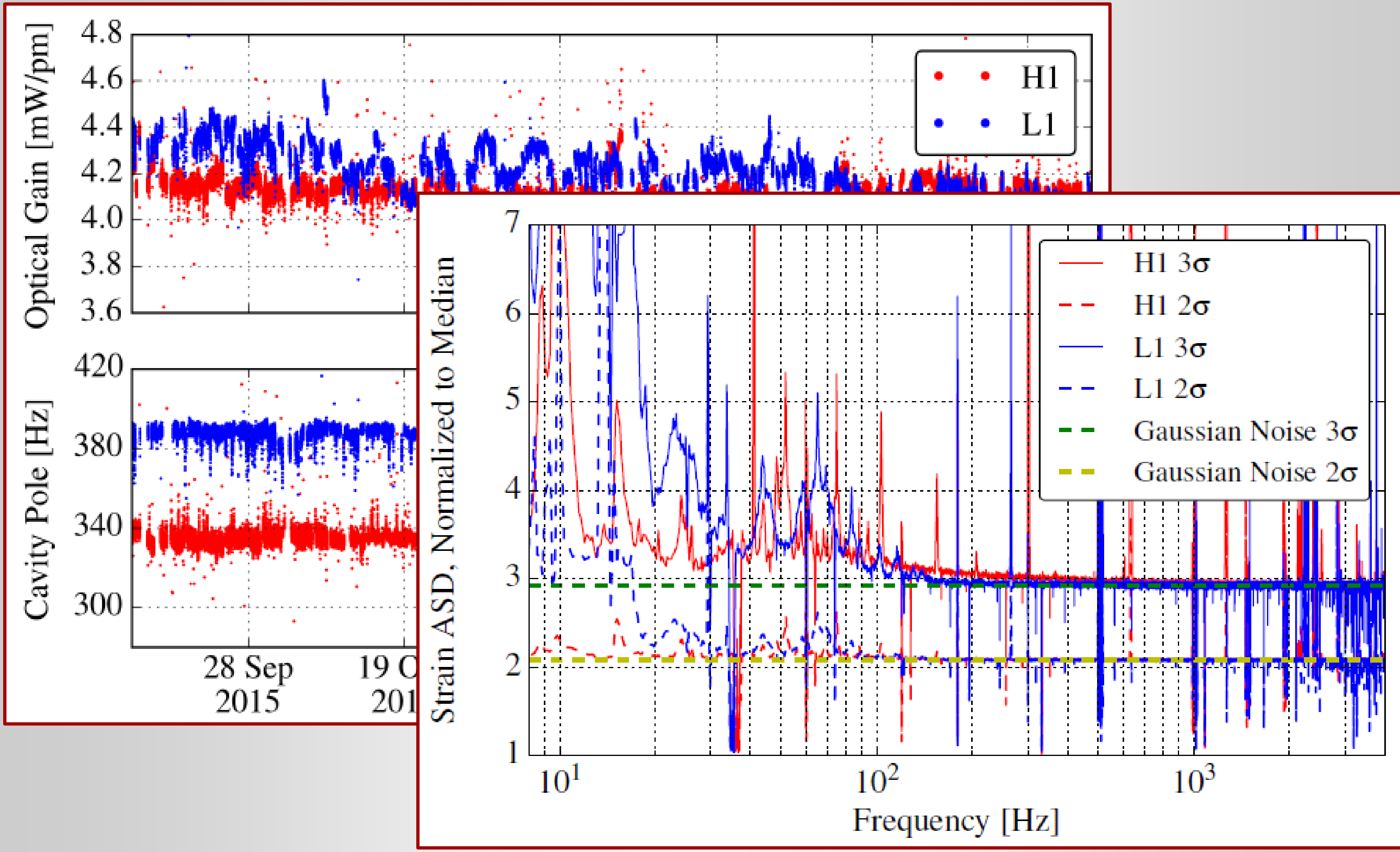

Martynov D.V. et al , arXiv:1604.00439 [astro-ph.IM]

Gravitational Wave Transducer

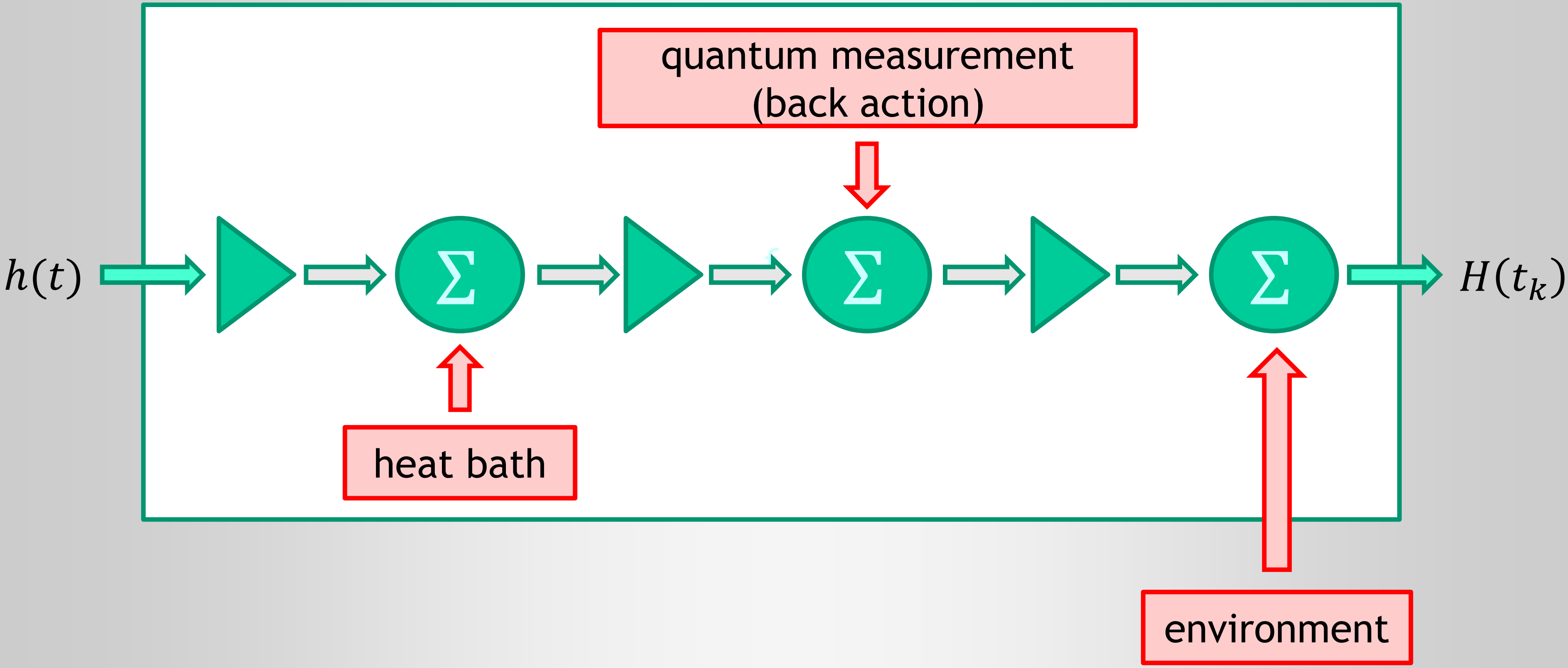

Near Future Developments

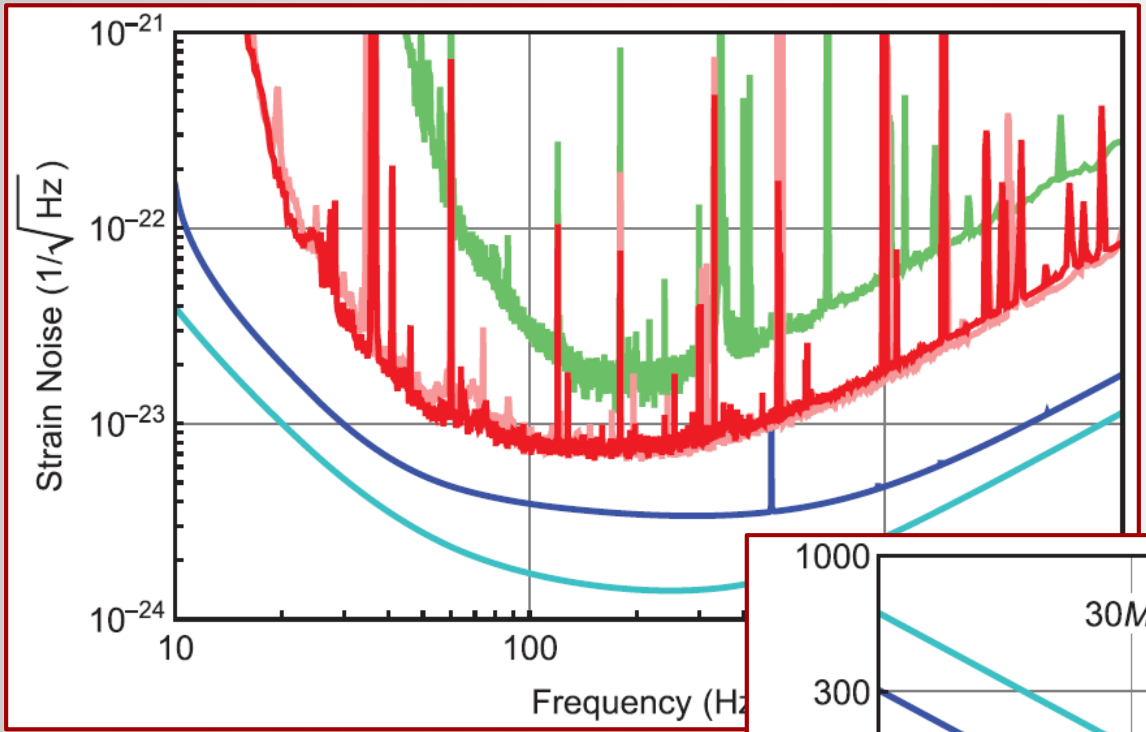

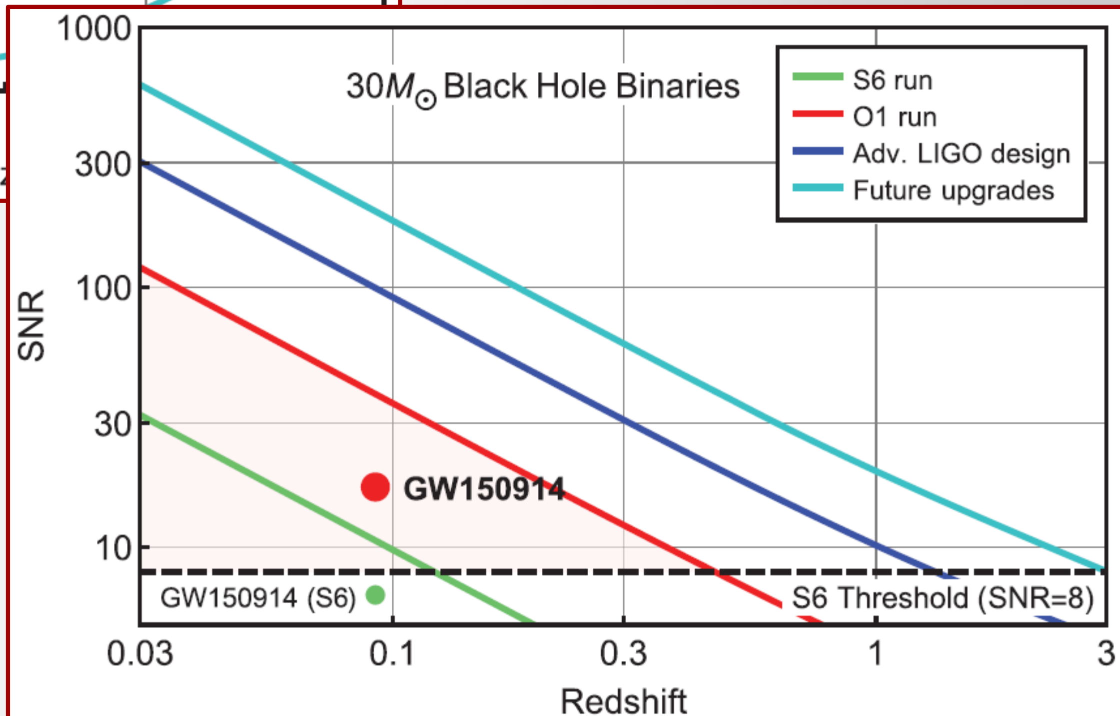

Leibniz Universität Hannover

Abbott et al. PRL 116, 131103 (2016), Miller et al. Phys. Rev. D 91, 062005 (2015)],

The Future of Gravitational Wave Detectors

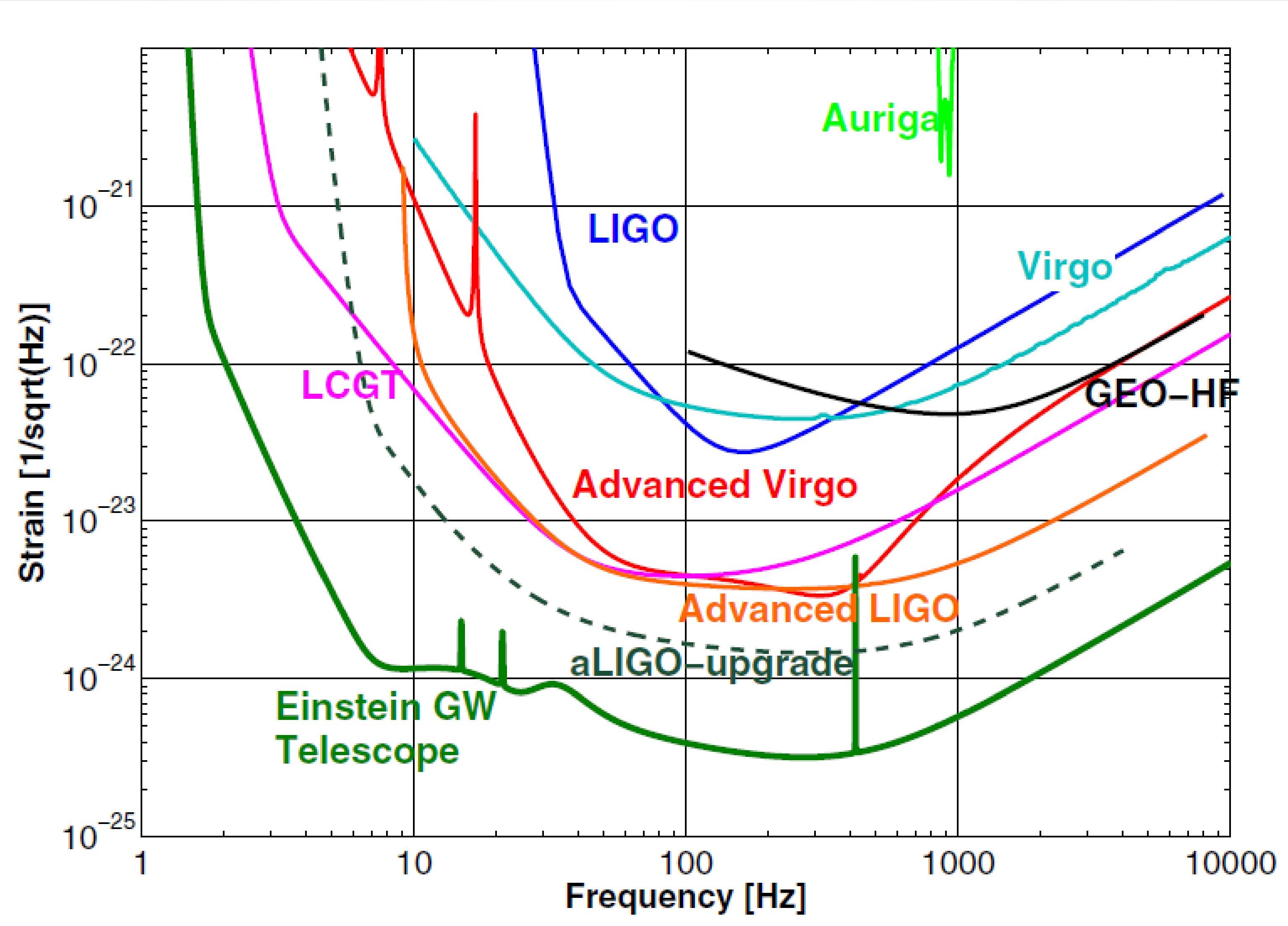

Hild S. Class. Quantum Grav. 29 (2012) 124006